Remarks

This application has been carefully reviewed in light of the non-final Office Action mailed October 30, 2008 (hereinafter "the Office Action"). At the time of the Office Action, claims 1-16 were pending the application. By this amendment, Applicants have amended claims 1, 11, 13, and 16 to recite with greater clarity that "the first and second catalyst are comprised of the identical catalyst material." In addition, claims 25-26 are newly added to further define that the "the first and second catalyst have the same carbon-deposition rate" and that "the first catalyst is presented with a lower fuel reforming rate compared to the second catalyst." Support for the amendment is found throughout the specification, and particularly at line 31 on page 2 to line 7 of page 3, lines 22 to 34 on page 3 of the specification. No new matter is introduced by this amendment. Moreover, the non-elected claims 17-24 have been canceled to expedite prosecution. In the Office Action, the Examiner rejected claims 1-16. Applicants respectfully request reconsideration of this application in view of the following remarks.

Claims 1-3, 6-8 and 13-15 stand rejected under 35 U.S.C. § 102(e) as being anticipated by Kaneko (JP 633,310,574, hereinafter *Kaneko*). Applicants respectfully request withdrawal of this rejection.

Independent claims 1 and 13 each recites a solid oxide fuel cell having an anode comprising *a single catalyst material* that promotes reforming dispersed within or upon a support structure such that the catalyst has a first concentration at a first position and a second concentration at a second position, wherein the first position is closer to the entrance (for the introduction of fuel to the solid oxide fuel cell) than the second position and the first concentration is lower than the second concentration.

As acknowledged by the Examiner on pages 3-4 of the Office Action, *Kaneko* teaches a solid oxide fuel cell having catalyst 8a and catalyst 8b illustrating "*plural kinds*" of oxide fuel cell catalysts, wherein the catalyst 8a is disposed upstream of the catalyst 8b in the direction of a fuel passage 12. Please see Abstract and Figure 1. (Emphasis added).

Contrary to the single catalyst material having differential catalyst concentration as recited in the independent claim 1 and claim 13, *Kaneko*'s catalyst 8a and catalyst 8b are different materials that perform drastically different tasks. As disclosed in the Abstract and in Figure 1, the catalyst 8b is the "usual" reforming catalyst, wherein the catalyst 8a, being accorded lower carbon deposition rate than the catalyst 8b, works to retard carbon deposition at the upstream side of the fuel passage 12, and as such, the fuel cell can be operated with improved cell performance.

Contrary to the assertions stated on page 3 of the Office Action, the difference in carbon deposition rate does not necessarily yield a difference in catalyst concentration, for the carbon deposition rate and the catalyst concentration are two different concepts within the context of oxide fuel cells.

Carbon deposition rate may relate to the formation of elemental carbon onto the surface of a catalyst and may be dependent on variables including the size of catalyst cluster, catalyst dispersion coordination, extent of reactant mixing, extent of catalyst sintering, metal vaporization, metal agglomeration, and the amount of steam going into the catalyst. Carbon deposition rate may also be affected by the nature of the catalyst metal, the chain length of the hydrocarbon fuel, C/H/O elemental ratio of the hydrocarbon fuel, and the temperature of the catalyst bed. Please see pages 2-3 of Exhibit 1, "Solid oxide fuel cell hybrid system for distributed power generation" by Nguyen Minh in July 2004 (pdf. copy attached and currently submitted for consideration via Information Disclosure Statement).[1] Please also see pages 6-7 of Exhibit 2, "2005 SECA Core Technology Review" by David A. Berry dated April 21, 2005 (pdf. copy attached).[2]

---

[1]   This   reference   is   available   via   the   following   site:
http://www.osti.gov/bridge/servlets/purl/897861-xGUTFu/ .

[2]   This reference is available via the following site:
http://www.netl.doe.gov/publications/proceedings/05/SECA_Workshop/pdf/day4/NETL-Berr
y%204-21.pdf.

On the other hand, the catalytic concentration of a solid oxide fuel cell catalyst generally relates to the properties of the catalyst as a reforming catalyst, for example, converting a hydrocarbon fuel to hydrogen and carbon monoxide (lines 1-5 on page 2 of the specification).

Just as in the case for carbon deposition rate, the catalyst concentration can also be affected by various parameters and is not strictly or directly related to the carbon deposition rate. By way of example, steam retention can be differentially retarded between two otherwise identically situated reforming catalysts if the two catalysts can be differentially surface treated, for example, to induce differential steam sensitivity while maintaining their catalytic concentration.

Kaneko fails to teach or suggest at least the aforementioned limitation recited in claims 1 and 13. The independent claims 1 and 13 and all the claims dependent therefrom are submitted to be patentable over *Kaneko*.

Claims 2-3, 6-8 and 4-5 are believed to be allowable for at least the same reasons stated above in relation to the independent claims 1 and 13 and further due to the additional features they recite. Separate and individual consideration is respectfully requested.

Anticipation has been held to be one of strict identity. The reference must expressly or implicitly teach every claimed limitation as recited in the subject claim(s). The fact that a certain result or characteristic may occur or be present in the prior art is not sufficient to establish the inherency of that result or characteristic. *In re Rijckaert*, 9F.3d 1531, 1534, 28 USPQ2d 1955, 1957 (Fed. Cir. 1993). To establish inherency, the extrinsic evidence "must make clear that the missing descriptive matter is ***necessarily*** present in the thing described in the reference, and it would be so recognized by persons of ordinary skill." *In re Oelrich*, 666 F.2d 578, 581-82, 212 USPQ 323, 326 (CCPA 1981). Please see also MPEP 2112.

As stated herein elsewhere, *Kaneko* does not mention at all differential catalyst concentrations, much less catalyst concentrations that change "monotonically" or "linearly" as respectively recited in the claims 2 and 3, respectively. Contrary to the assertions stated on page

4 of the Office Action, *Kaneko* does not teach catalyst concentration that changes "gradually." At best *Kaneko* teaches an oxide fuel cell having two or more different kinds of catalysts with different carbon-deposition rates and performing different tasks. There is no teaching as to the comparative relationship between the catalyst concentrations of the catalyst 8a and the catalyst 8b, much less the relationship being one of "gradually" changing as proposed by the Examiner. As such, different catalyst concentration or particularly catalyst concentration that change "monotonically" or "linearly" is neither expressly taught by nor necessarily present in *Kaneko*. Patentability of claims 2 and 3 are solicited at least on this independent ground.

Claims 4-5, 9-10 and 12 stand rejected under 35 U.S.C. § 103(a) as being unpatentable over *Kaneko*. Applicants traverse this rejection because *Kaneko* does not teach or suggest the pending claims 4-5, 9-10 and 12. Claims 4-5, 9-10 and 12 depend from the independent claim 1. As set forth above, *Kaneko* does not teach or suggest the aforementioned limitation of claim 1 with respect to the differential catalyst concentration within the same reforming catalyst. Claims 4-5, 9-10 and 12 which depend from claim 1, are believed to be patentable for at least the same rationale set forth above in relation to the independent claim 1 and further due to the additional features they recite. Separate and individual consideration is respectfully requested.

MPEP 2142 in relevant portions provides:

> The key to supporting any rejection under 35 U.S.C. § 103 is the ***clear articulation of the reason(s)*** why the claimed invention would have been obvious. The Supreme Court in *KSR International Co. Teleflex Inc.*, 82 USPQ2d 1385, 1396 (2007) noted that the analysis supporting a rejection under 35 U.S.C. § 103 ***should be made explicit***. The Federal Circuit has stated that "rejections on obviousness ***cannot be sustained with mere conclusory statements; instead, there must be some articulated reasoning with some rational underpinning*** to support the legal conclusion of obviousness." *In re Kahn*, 441 F.3d 977, 988, 78 USPQ2d 1329, 1336 (Fed. Cir. 2006).

MPEP in relevant portion further provides:

> After indicating that the rejection is under 35 U.S.C. § 103, the ***examiner should set forth*** in the Office action:

> (A)   *the relevant teachings of the prior artrelied upon,*
> *preferably with reference to the relevant column or page number(sw) and line*
> *(numbers) where appropriate, ...*
>
> (D)   *an explanation >as to<why> the claimed invention would*
> *have been obvious to <one of ordinary* skill in the art at the time the invention
> was made.
> "To support the conclusion that the claimed invention is directed
> to obvious subject matter, *either the references must expressly or impliedly*
> *suggest the claimed invention or the examiner must present a convincing line*
> *of reasoning as to why the artisan would have found the claimed invention to*
> *have been obvious* in light of the teachings of the references." *Ex parte Clapp*,
> 227 USPQ 972, 973 (Bd. Pat. App. & Inter. 1985).

In light of the above-cited MPEP provisions and with the reasons given below, Applicants respectfully submit that claim rejections stated on Pages 4-5 of the Office Action are merely conclusory and have failed to set forth "articulated reasoning with some rational underpinning, and as such, fails to establish a *prima facie* case of obviousness.

In rejecting claims 4-5, 9-10 and 12 under 35 U.S.C. § 103(a) over *Kaneko*, the Examiner acknowledges that *Kaneko* "does not expressly disclose" respective claimed limitations in the subject claims, yet maintains that the claims are nevertheless obvious by stating rather conclusively that "it would have been obvious to one having ordinary skill in the art at the time the invention was made to employ the instant catalytic concentration" and that "it is well within the artisan skill to vary the catalyst concentration across the fuel cell channel through routine experimentation."

As illustrated above, it is clear that other than simply repeating what is recited in the claims, the instant rejections under 35 U.S.C. § 103(a) provide no articulated reasoning as to the obviousness, let alone factual findings in *Kaneko* that would support the rejections, as otherwise required in establishing a *prima facie* case of obviousness under MPEP 706.02(j) and MPEP 2142 cited above.

Moreover, the "routine experimentation" simply does not apply here. The "routine experimentation" doctrine as interpreted by the Patent Office refers to a situation "where the

general conditions of a claim are disclosed in the prior art, it is not inventive to discover the optimum or workable ranges by routine experimentation." MPEP 2144.05 in relevant portions. Please also see *In re Aller*, 220 F.2d 454, 456, 105 USPQ 233, 235 (CCPA 1955).

The Examiner has agreed that *Kaneko* does not teach the various claimed limitations of the subject claims (pages 4-5 of the Office Action). In fact, *Kaneko* does not appear to either teach any "general conditions" of the various claimed limitations, or any "optimum or workable ranges" thereof. This lack of teaching is further compounded by the fact that *Kaneko* fails even to teach catalytic concentrations as stated above.

Simply put, when there is no teaching in the art about the general condition of how best to compensate temporary thermal damages within the context of oxide fuel cell by employing differential reforming catalyst concentrations as recited in claim 1, there would exist no basis to experiment on, let alone to "routinely" experiment on.

For the similar token, the cited "*In re Boesch*" with respect to "result effective variable" would not be applicable here to render obvious the claimed limitation of the catalyst amount of 1 to 50%.

A particular parameter must first be recognized as a result-effective variable, i.e., a variable which achieves a recognized result, before the determination of the optimum or workable ranges of said variable might be characterized as routine experimentation. MPEP 2144.05(II)

Unlike *In re Boesch* wherein prior art did in fact have suggested proportional balancing as a result-effective variable to achieve desired results in the formation of an alloy, the art in the present case has not suggested the differential concentration of a catalyst for an oxide fuel cell as a "result effective variable," to promote the ultimate effect of fuel reforming wherein thermal challenges may be rendered.

Taken together, Applicant respectfully submits that a *prima facie* case of obviousness has not been established in the subject rejections. Reconsideration and withdrawal of the rejections to claims 4-5, 9-10 and 12 under 35 U.S.C. § 103(a) over *Kaneko* is solicited.

Claims 11 and 16 stand rejected under 35 U.S.C. § 103(a) as being unpatentable over *Kaneko* and Sridhar, et al. (U.S. 2005/0074650) hereinafter *Sridhar*. Applicants traverse this rejection because the proposed combination does not teach or suggest pending claims 11 and 16. Claims 11 and 16 depend respectively from the independent claims 1 and 13. As set forth above, *Kaneko* does not teach or suggest that the differential catalyst concentration as recited in claim 1 or 13. *Sridhar* does not cure the defection teachings of *Kaneko*. Moreover, the Examiner has not set forth how *Sridhar* would cure the defective teachings in view of the above. In fact, *Sridhar* does not even mention catalyst concentration of precious metals, let alone the aforementioned limitation as recited in claims 1 and 13. For at least this reason, claims 11 and 26 which depend from claims 1 and 13, are patentable over the proposed combination of *Kaneko* and *Sridhar*.

Claims 25-26 are added new to further define the solid oxide fuel cell of claim 1 wherein "the first and second catalyst have the same carbon-deposition rate" or wherein "the first catalyst is presented with a lower fuel reforming rate compared to the second catalyst." Claims 25-26 are believed to be patentable over the prior art and patentability thereof is respectfully solicited.

Applicants do not acquiesce in the Examiner's characterizations of the art. For brevity and to advance prosecution, Applicants may not have addressed all characterizations of the art and reserve the right to do so in further prosecution of this or a subsequent application. The absence of an explicit response by Applicants to any of the Examiner's positions does not constitute a concession to the Examiner's positions. The fact that Applicants' comments have focused on particular arguments does not constitute a concession that there are not other arguments for patentability of the claims. Applicants submit that all of the dependent claims are patentable for at least the reasons given with respect to the claims on which they depend.

For the foregoing reasons, Applicants believe that the Office Action of October 30, 2008, has been fully responded to. Consequently, in view of the above amendments and remarks, Applicants respectfully submit that the application is in condition for allowance, which allowance is respectfully requested.

The Examiner is requested to telephone Applicant's attorney if it would advance the prosecution of this application.

Respectfully submitted,

Kevin Ellwood et al.

By /Junqi Hang/
    Junqi Hang
    Reg. No. 54,615
    Attorney for Applicant

Date: January 29, 2009

BROOKS KUSHMAN P.C.
1000 Town Center, 22nd Floor
Southfield, MI 48075-1238
Phone: 248-358-4400
Fax: 248-358-3351

EXHIBIT 1

Solid Oxide Fuel Cell Hybrid System for Distributed Power Generation

Semi-Annual Technical Progress Report
January 2004 to June 2004

Nguyen Minh

Principal Investigator

July 2004

Performed under DOE/NETL Cooperative Agreement
DE-FC26-01NT40779

GE Hybrid Power Generation Systems

19310 Pacific Gateway Drive

Torrance, CA 90502

Disclaimer

Abstract

This report summarizes the work performed by Hybrid Power Generation Systems, LLC (HPGS) during the January to June 2004 reporting period under Cooperative Agreement DE-FC26-01NT40779 for the U. S. Department of Energy, National Energy Technology Laboratory (DOE/NETL) entitled "Solid Oxide Fuel Cell Hybrid System for Distributed Power Generation". The main objective of this project is to develop and demonstrate the feasibility of a highly efficient hybrid system integrating a planar Solid Oxide Fuel Cell (SOFC) and a micro-turbine. In addition, an activity included in this program focuses on the development of an integrated coal gasification fuel cell system concept based on planar SOFC technology. Also, another activity included in this program focuses on the development of SOFC scale up strategies.

Table of Contents

List of Figures

List of Tables

Executive Summary

During this reporting period the phase 1 SOFC barrier resolution task was successfully completed. In particular, the experimental work related to the impact of pressure on cell performance degradation and the carbon formation boundary was completed.

A number of SOFC module tests have been completed to evaluate the pressure impact to performance stability. The results show that the operating pressure accelerates the performance degradation. The potential causes of the performance decay include oxidation of the metal interconnect, chromium poisoning to electrodes, interface resistance increase, electrode microstructure changes, back diffusion/leakage, and/or electrode conditioning process. The dominant degradation mechanisms remain unclear. Both interconnect oxidation and Cr transport to cathode were evident based in post-test analysis. To reduce the degradation related to metallic interconnect, interconnect materials have to be improved or protected with a coating. Future work is needed to understand the degradation mechanisms and the impact of pressure on the electrode conditioning processes.

Several experiments were conducted to explore the effects of pressure on carbon formation. While carbon formation is favored at pressurized conditions, the conditions at which carbon formation occurs in a functioning cell is difficult to predict. Experimental observations on a functioning cell have verified that carbon deposition does not occur in the cell at steam-to-carbon ratios lower than the steady-state design point for hybrid systems. These results are in good agreement with theoretical analysis. These experiments were conducted on 3-inch and 4 3/8-inch SOFC cells operating at 4 atmospheres.

At the start of this reporting period the subscale demonstration system task was terminated. This effort was concluded with the review of several system concepts and the downselection of a single system concept for detailed analysis. The results of this effort has been detailed in the previous report. In lieu of the subscale demonstration system activities, the stack hybridization task was initiated. .

Finally, activities on the SOFC Scale-up task continued. A functional product specification was completed. Several concepts were brainstormed and distilled down to four concepts. Preliminary cost, reliability, and performance models were constructed for these concepts. The results from these models were used to downselect to a single concept for further analysis.

Experimental

All experimental work currently performed on the program is contained in sub-task 1A.2.2, Barrier Resolution -- Pressurized SOFC. The test procedures and the test methods used to perform the experimental work for this task have been described in previous Quarterly Technical Progress Reports. Experimental methods currently being

developed for carbon deposition testing are described and discussed in the section 1.1.1, titled Carbon Deposition Experiments.

Results and Discussion

1   TASK 1A.2 – TECHNICAL BARRIER RESOLUTION

1.1   Subtask 1.A.2. 2 – Pressurized SOFC

Single cell pressurized testing has been performed using two identical pressure vessels that have a stamped vessel rating for 60 psig. These vessels have been used to conduct pressurized carbon deposition experiments and performance degradation or life tests.

1.1.1   Carbon Deposition Experiments

The use of nickel based anode has many advantages over others in terms of cell support structure (anode-supported cells), fast electrochemical oxidation kinetics (high exchange current density) and high activity toward reformation of fuels (internal reforming of hydrocarbon fuels). Especially, the high internal reforming activity provided by nickel based anodes allows highly efficient cell operation with reduced degree of external reformation, leading to a smaller external reformer. However, one concern with the use of hydrocarbon containing fuel streams is carbon deposition. The problem of carbon deposition is present whenever hydrocarbon containing fuel is employed as anode fuel irrespective of pre-reformation method (such as steam, auto-thermal or partial oxidation reformation).

Carbon deposition is generally observed over non-noble metal catalysts such as Ni, Co and Fe. The carbon deposition rate is impacted by many factors, such as the nature of the catalyst material, the chain length of hydrocarbon fuels, carbon/hydrogen/oxygen (C/H/O) elemental ratio of the fuel stream, and temperature and residence time. Also, the nature of carbon that is deposited (whether it is nanotube, whisker, polymeric, etc..) is dependent on the above mentioned reaction conditions.   Generally, higher hydrocarbon fuels exhibit considerably higher rates of carbon deposition.

A fuel stream that shows high carbon element percentage in its C/H/O elemental ratio shows higher thermodynamic driving force toward carbon deposition. Therefore, raising the H and/or O ratio in C/H/O elemental ratio helps to prevent or circumvent environments that lead to carbon deposition. This directly translates to adding more steam or oxygen (or air) to the anode fuel stream for either external or internal reformation.   During fuel cell operation, the generation of current is equivalent to transferring oxygen from the cathode stream to the anode stream through the electrolyte. Therefore, the fuel stream composition changes gradually as it travels along the anode flow field. The anode inlet of the cell corresponds to zero current generation and therefore, is more likely susceptible to carbon deposition. Contrarily, fuel stream leaving the anode flow field is relatively rich in O in its elemental C/H/O ratio and

2

therefore, it is far less likely to suffer from carbon deposition, or in other words, is far away from carbon deposition boundary.

The thermodynamic prediction of carbon deposition at 1 atm in a cell running on a simple mixture of methane and steam is depicted in Figure 1. The elemental compositions of the individual anode fuel streams were calculated and plotted in elemental ternary diagram. Also, the composition of anode fuel stream that went through 80% fuel utilization was calculated and plotted on the diagram for comparison. The carbon boundary line shown in Figure 1 was reproduced from literature and it was found to agree well with our thermodynamic calculations. From Figure 1, anode fuel stream of S/C 1.5 (i.e. a simple mixture of H_2O and CH_4 in the ratio of 1.5) is located far below the carbon boundary at 800°C both at the anode inlet and outlet locations, with fuel utilization at 80%. This implies that all anode regions are safe from carbon deposition. Contrarily, the inlet region of S/C 0.1 anode fuel stream is located above the carbon boundary indicating potential for carbon deposition.

As shown in Figure 1, the elemental ratio of C/H/O changes along the anode flow field such that it can cross the carbon deposition boundary. Moreover, the accompanying internal reforming reaction, aside from current generation, contributes to local temperature changes since the internal reformation reaction is strongly endothermic. These factors make the prediction of carbon deposition in a working fuel cell complicated. In addition, kinetic factors are not taken into account in this thermodynamic prediction. Therefore, it is imperative to experimentally verify the conditions under which fuel cells can be run on hydrocarbon fuels (methane in this study) without the risk of carbon deposition.
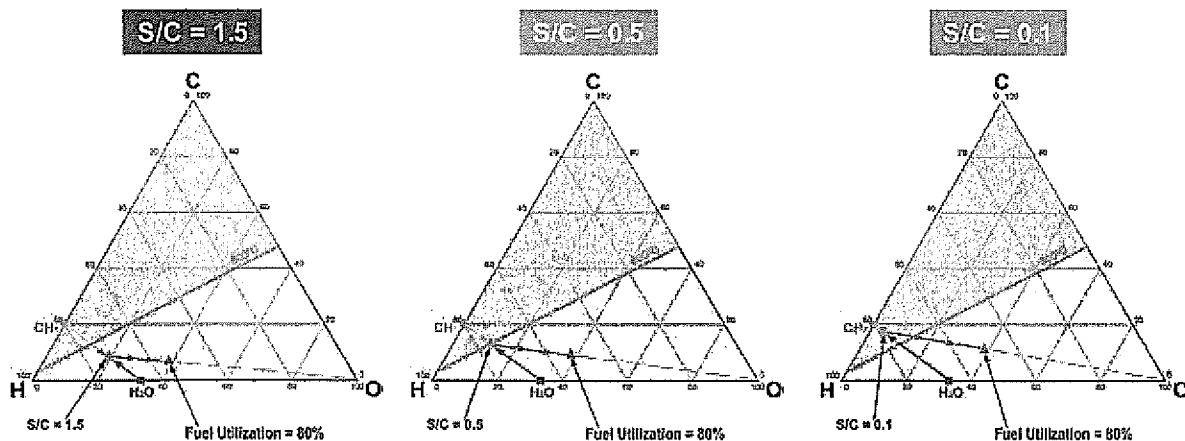

Figure 1: Carbon deposition prediction in fuel cell anode

In this study, the potential degradation of cell performance associated with carbon deposition was experimentally evaluated for both ambient and elevated pressure (44.1 psig). Single cell modules with interconnects operating on a controlled reformate

3

composition were employed and the effect of carbon deposition was observed based on cell performance and stability.

1.1.1.1 Testing Approach

In this task, cells were operated on a number of controlled anode fuel streams and the cell performance was monitored to learn the effect of carbon deposition on cell performance and stability. The cell performance test was conducted at a constant cell load (current) and cell voltage was measured. A drop in cell voltage over time is attributed to carbon deposition over the anode electrode if it exceeds the expected steady state degradation.

Experiments were conducted using 3-inch and 4 3/8-inch circular cells with a sealless radial flow field configuration. In this configuration the anode fuel stream and cathode air stream exhausts were mixed together and combusted inside the vessel after leaving the cell. Once the cell was assembled, mounted and plumbed for gas feed, it was reduced at two different conditions (25% H2 and 64% H2, respectively) for a predetermined period of time. Then, the cell was conditioned for its maximum performance by applying an electric load for about 20 hours. Once the cell exhibited acceptable performance through cell conditioning, cell testing with a number of simulated anode fuel stream was initiated. At the start of the test the anode fuel stream was wet enough (corresponding to high steam-to-carbon ratio of fuel stream) to ensure that carbon deposition did not occur. During this period the performance and stability of the cell was monitored for a predetermined period of time. Once the cell demonstrated stable operation with the "wet" fuel stream, the anode stream was transitioned to a "drier" (corresponding to low steam-to-carbon ratio) fuel composition and the cell performance and stability was monitored. This process was repeated until cell voltage drop attributed to carbon deposition was observed. The voltage was allowed to continue dropping for a prescribed period of time or until the voltage got as low as 0.55V. This was to ensure that sufficient carbon was deposited for verification purposes. Finally, the cell was put under open circuit condition (with no electric load) and subsequently cooled down under a controlled environment to preserve any carbon deposits. Subsequently, carbon deposits were verified through microscopic surface analysis.

1.1.1.2 Test Set-Up

The testing for carbon deposition was designed to mimic a cell operating within the framework of a hybrid system configuration as shown in Figure 2. Upstream of the cell, methane and steam, with a predetermined steam-to-carbon ratio, is mixed with the anode exhaust recycle stream. Then, this mixture flows through the "Steam Reformer" and "SOFC, Anode" for external steam reformation and power generation, respectively. The anode exhaust out of "SOFC, Anode" is then split into two directions. Part of the anode exhaust stream is directed out of the system for further processing and the other part of the anode exhaust stream is recycled back to the inlet fuel. A closer look at the system configuration reveals that the composition of the anode fuel stream that enters

4

the "SOFC, Anode" is determined by many system design factors, such as steam-to-carbon ratio in the inlet fuel mixture, the steam reformer size and temperature, the cell current density and fuel utilization, and the anode exhaust recycle ratio. In determining system representative anode fuel stream compositions, cell current density and fuel utilization were set at 400mA/cm2 and 80%, respectively. Steam-to-carbon ratio was found to be a major factor that determines the anode fuel stream composition and representative values of steam reformer size/temperature and anode exhaust recycle ratio were used in the calculation of anode fuel stream composition.
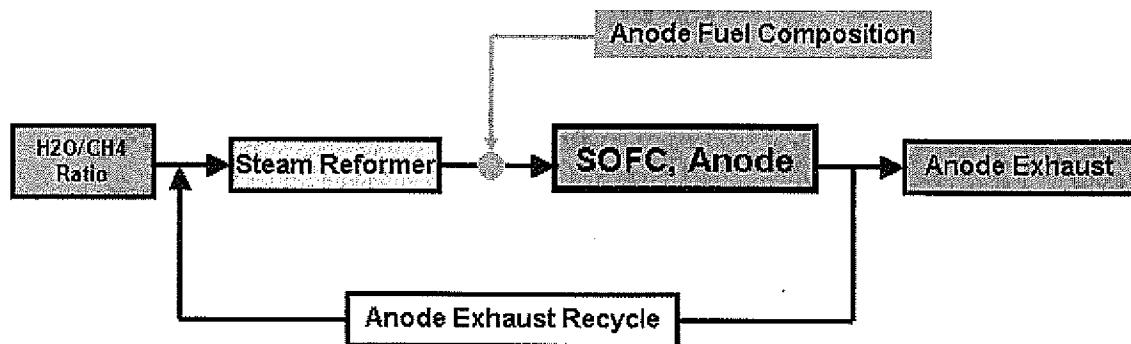

Figure 2: Configuration of fuel cell within the framework of hybrid system design

The anode fuel stream composition was computed using the process described above and calculated using process modeling software and is summarized in Table 1.

S/C	3.0	2.0	1.5	1.0	0.7	0.6	0.5	0.4	0.3	0.2	0.1	0.001
H_2	26.3%	28.6%	30.0%	31.5%	32.0%	32.2%	32.0%	31.9%	31.1%	30.0%	26.6%	4.0%
O_2	0.0%	0.0%	0.0%	0.0%	0.0%	0.0%	0.0%	0.0%	0.0%	0.0%	0.0%	0.0%
H_2O	36.3%	31.4%	27.6%	22.2%	17.8%	15.7%	13.8%	11.3%	8.5%	5.0%	1.2%	0.0%
N_2	0.0%	0.1%	0.1%	0.1%	0.0%	0.0%	0.0%	0.0%	0.0%	0.0%	0.0%	0.0%
CO_2	24.0%	21.7%	19.7%	16.7%	13.9%	12.6%	11.3%	9.4%	7.4%	4.5%	1.0%	0.0%
CH_4	6.0%	10.0%	13.6%	19.4%	25.3%	28.0%	31.3%	35.2%	40.6%	47.4%	58.3%	92.6%
CO	7.3%	8.3%	9.1%	10.2%	11.0%	11.4%	11.6%	12.1%	12.4%	13.0%	12.9%	0.2%
C_2H_6												2.8%
Total	100.0%	100.0%	100.0%	100.0%	100.0%	100.0%	100.0%	100.0%	100.0%	100.0%	100.0%	99.7%

Table 1: Anode fuel stream composition at different steam-to-carbon ratios

Overall, the anode fuel stream composition is enriched with methane, while the steam content drops as steam-to-carbon ratio decreases. The elemental composition corresponding to individual steam-to-carbon ratios was calculated based on the anode fuel stream composition in Table 1 and is listed in Table 2.

S/C	3.0	2.0	1.5	1.0	0.7	0.6	0.5	0.4	0.3	0.2	0.1	0.001
C	13.4%	14.1%	14.7%	15.6%	16.3%	16.7%	17.0%	17.4%	17.9%	18.5%	19.1%	19.9%
H	53.7%	56.5%	58.9%	62.3%	65.3%	66.6%	68.0%	69.6%	71.6%	73.8%	76.6%	80.0%
O	32.9%	29.3%	26.4%	22.1%	18.4%	16.7%	15.0%	13.0%	10.5%	7.7%	4.2%	0.0%
Total	100.0%	100.0%	100.0%	100.0%	100.0%	100.0%	100.0%	100.0%	100.0%	100.0%	100.0%	100.0%

Table 2: Elemental composition of anode fuel stream at different steam-to-carbon ratios

A schematic of test set-up for pressurized carbon deposition experiment is shown below in Figure 3.
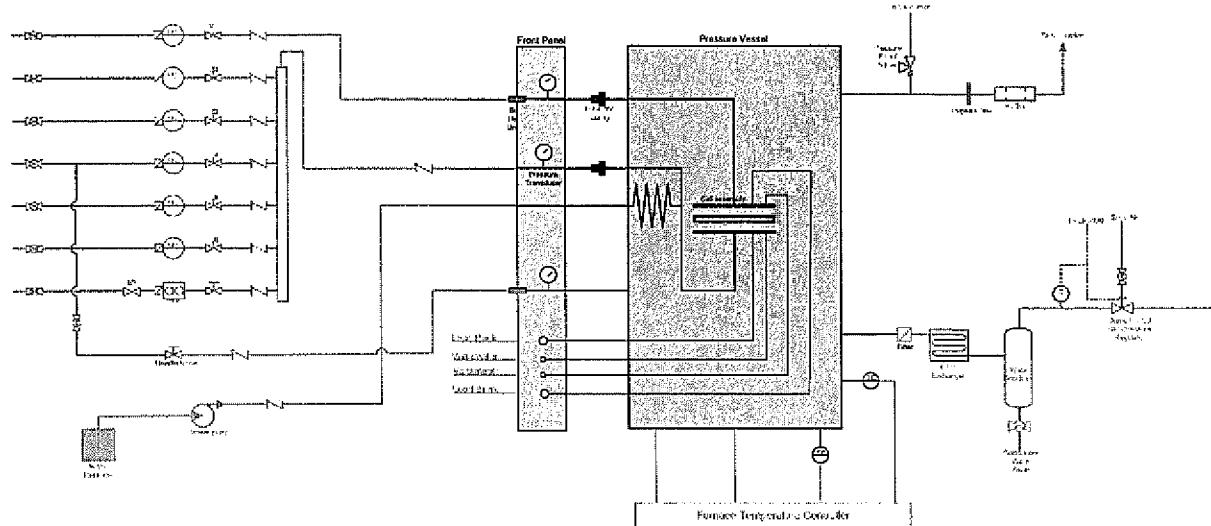
Figure 3: Schematic of test set-up for pressurized carbon deposition experiments

A single cell module was housed inside a cylindrical pressure vessel, equipped with an electrical furnace for heating up of the cell module. Programmable temperature controllers were employed for precise and programmed temperature control of the vessel. Mass flow controllers were used for precise and controlled flow rates of individual fuel gases. These individual gas flows were mixed and then introduced to the anode flow field. The anode fuel stream was preheated as it travels through the fuel preheating line in the vessel. A separate water line from the liquid water pump entered the vessel and steam was generated as it traveled through the coiled water preheating line before entering the anode fuel preheating line as shown in Figure 3. Radial seal-less single cell SOFC modules of 3-inch diameter were used for ambient pressure experiments while 4 3/8-inch radial seal-less single cell SOFC modules were used for pressurized (44.1 psig) experiments. With the radial seal-less cell module, excess fuel in the anode exhaust stream that had not been consumed at the anode was combusted along the circumference of the cell. This helped to maintain the overall cell temperature. For pressurized tests, a back pressure regulator was employed to

pressurize the cell. For safety purposes, the pressure vessel was equipped with a pressure relief valve. The pressure relief valve opened up to prevent any excessive and accidental pressure build-up inside the vessel. The test set-up was interfaced with a digital data acquisition system that loged time stamped information such as individual gas flows, temperature, cell voltage and current. A pressure transducer was installed upstream of the fuel preheating line outside the furnace and pressure vessel and the pressure in the fuel line was monitored to ensure there is no flow blockage.

1.1.1.3 Test Results

1.1.1.3.1 Ambient Pressure Experiments

Altogether, 10 cells were assembled and tested for carbon deposition experiments at ambient pressure during this reporting period. Initial tests were used for verifying and troubleshooting the test setup, and for rough mapping of the carbon deposition regions. Later tests were used to pinpoint the carbon deposition regions.

Figure 4 shows cell voltage and upstream fuel line pressure plotted as a function of time for different anode fuel stream compositions. As specified above, the cell was first reduced and then conditioned at 457 mA/cm^2 for 20 hours. This conditioning procedure increased cell voltage from 0.617V to 0.670V. Following the cell conditioning, the anode fuel stream was transitioned to a steam-to-carbon ratio of 1.0, with fuel composition as specified in Table 1. In previous cell tests, stable cell performance on steam-to-carbon ratio of 1.5 (S/C 1.5) had been demonstrated several times and so it was considered safe to start at this condition to establish stable operation without carbon deposition after cell conditioning.   The total anode fuel flow rate after the cell conditioning was controlled throughout the whole test period to maintain fuel utilization of 28.6% at current density of 286mA/cm^2 at an operating cell voltage above 0.7V.
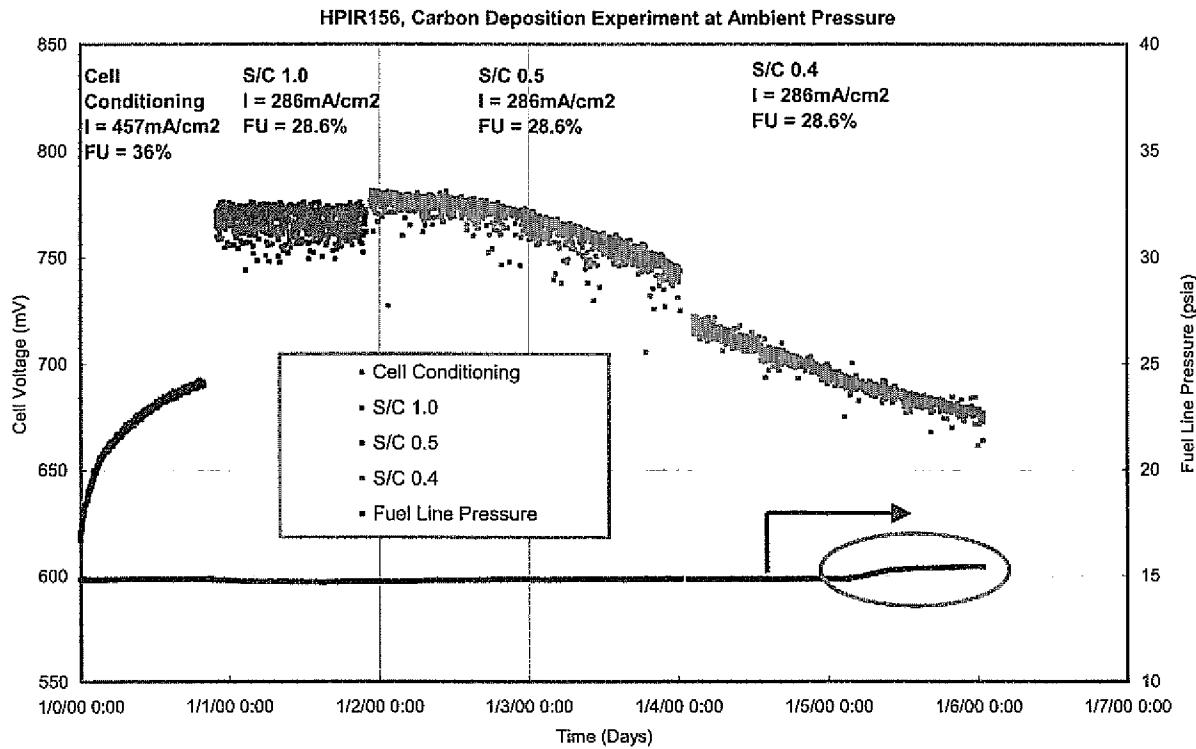
Figure 4: Carbon deposition experiment result at ambient pressure

As shown in Figure 4 the cell maintained stable cell voltage of 0.77 ± 0.015 V for 24 hours at anode fuel stream S/C of 1.0. Fluctuations in cell voltage was observed generally on cells running on reformate fuel streams containing steam. These fluctuations were caused by fluctuations in the steam generation for the test. The degree of voltage fluctuation was experimentally observed to be higher as the anode fuel stream was enriched with steam.

After reaching 24 hours of cell operation on S/C 1.0 anode fuel stream, anode fuel stream was transitioned to S/C 0.5. At this condition the cell showed very slow and gradual voltage drop without increase in fuel line pressure, indicating carbon deposition on the cell. The cell voltage dropped from 0.777V to 0.769V over 24 hours (voltage drop rate 0.333mV/hr). The cell was subsequently operated for a second 24 hours duration on S/C 0.5 anode fuel stream. The cell voltage continued to drop gradually (from 0.769V to 0.743V) but at an increased rate of 1.08mV/hr. As the cell voltage drop rate measured was fairly low and the cell voltage remained above 0.7V, even after 48 hours of cell operation on S/C 0.5, it was decided to reduce the steam content further to S/C 0.4 for an extended period of time (another 48 hours) as shown in Figure 4. The cell voltage drop rate on S/C 0.4 anode fuel stream for 48 hours was measured to be approximately 0.90mV/hr and this rate was very close to the one measured on S/C 0.5 anode fuel stream. A slight increase in the fuel line pressure was observed (from 14.9

8

psia to 15.4 psia) while the cell was operated on S/C 0.4 anode fuel stream. The fuel line pressure rise was later found to be due to the clogging of the dry fuel line upstream of the steam mixing point due to carbon deposition. The amount of carbon left inside the fuel preheating line was measured and assuming that the carbon deposition inside the fuel preheating line occurred for 48 hours, it corresponded to less 2% of methane flow rate in S/C 0.5 anode fuel stream. As the fuel utilization level in this experiment was low (28.6%), methane consumed for carbon deposition in the fuel preheating line was considered to have very minimal effect on cell voltage drop observed on S/C 0.5 and 0.4 anode fuel stream.

The cell was cooled down after reaching 48 hours of operation on S/C 0.4 anode fuel stream and the cell assembly was removed from cell stand and the cell was tore open from the endplates to inspect for any changes in cell structure or to locate any carbon deposits that may have been formed over the anode flow field or the cell anode surface.

Figure 5 shows an image of cell anode after the conclusion of the ambient test described above. It appears that the anode is in a reduced state (gray color of metallic nickel) and no carbon species were visually found. The small black powder along the edge of anode cell pieces in Figure 5 is cathode material.
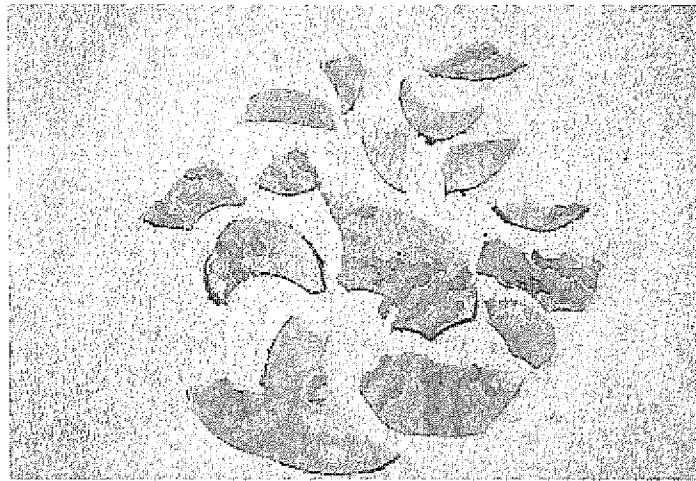
Figure 5: Image of cell anode taken out after carbon deposition experiment at ambient pressure

The cell anode was further inspected using SEM-EDX surface analysis techniques. Various points across the anode layer were inspected. Figure 6 shows a typical SEM-EDX spectrum obtained from the cell anode of Figure 5. A small C peak is present in the spectrum on both YSZ (left) and Ni (right) particles. Anode with visible carbon deposit is reported to yield a C peak that is comparable in size to the Zr peak. Considering the little C peak on SEM-EDX spectrum in Figure 6, the carbon deposition was considered to occur fairly slowly on both S/C 0.5 and 0.4 anode fuel streams and

that slow carbon deposition rate resulted in low cell voltage drop rate as shown in Figure 4.
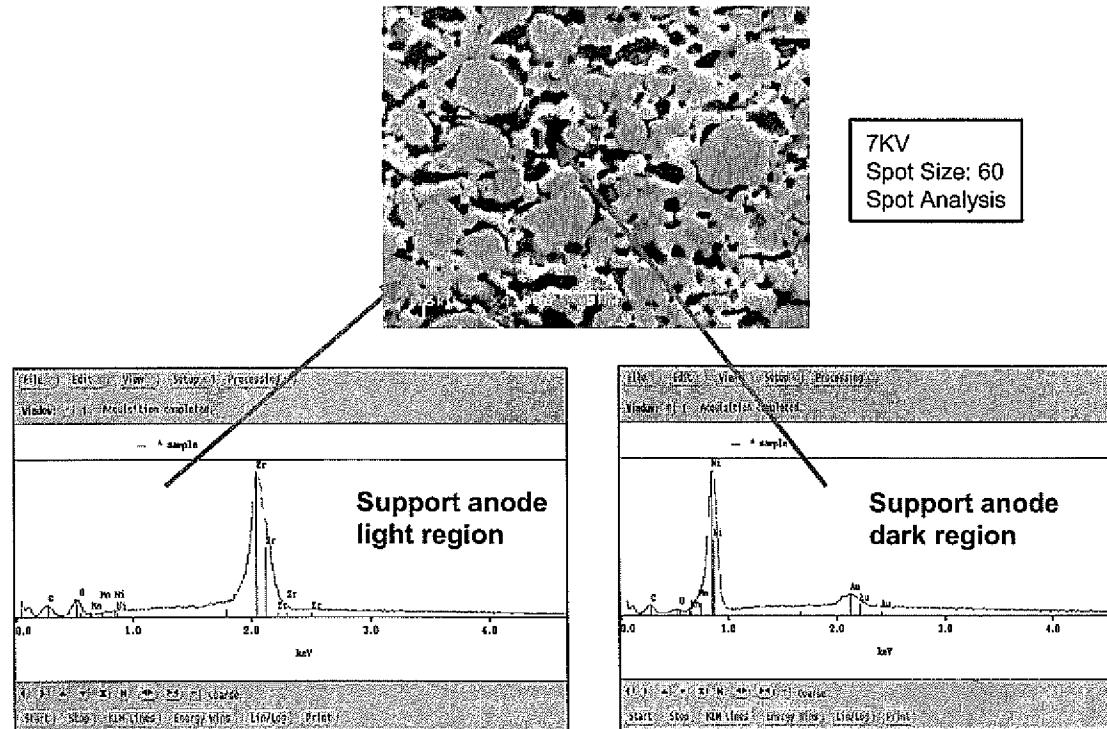

Figure 6: SEM-EDX spectrum taken from anode support layer after carbon deposition experiment at ambient pressure

Thermodynamic calculations predict that the carbon deposition boundary lies between S/C 0.6 and S/C 0.7 anode fuel stream composition of Table 1 at ambient pressure and 800°C. The results of the experiment (carbon deposition at S/C of 0.5 and 0.4) are consistent with the thermodynamic calculations.

1.1.1.3.2 Elevated Pressure (44.1 psig) Experiments

Two pressurized tests were conducted on 4-3/8 inch circular seal-less SOFC single-cell modules. The assembled cell went through cell reduction and cell conditioning before pressurization. The cell voltage and fuel line pressure data collected during this test is shown in Figure 7.

Cell 183-5, Carbon Deposition Experiment at Elevated Pressure (44.1 psig)
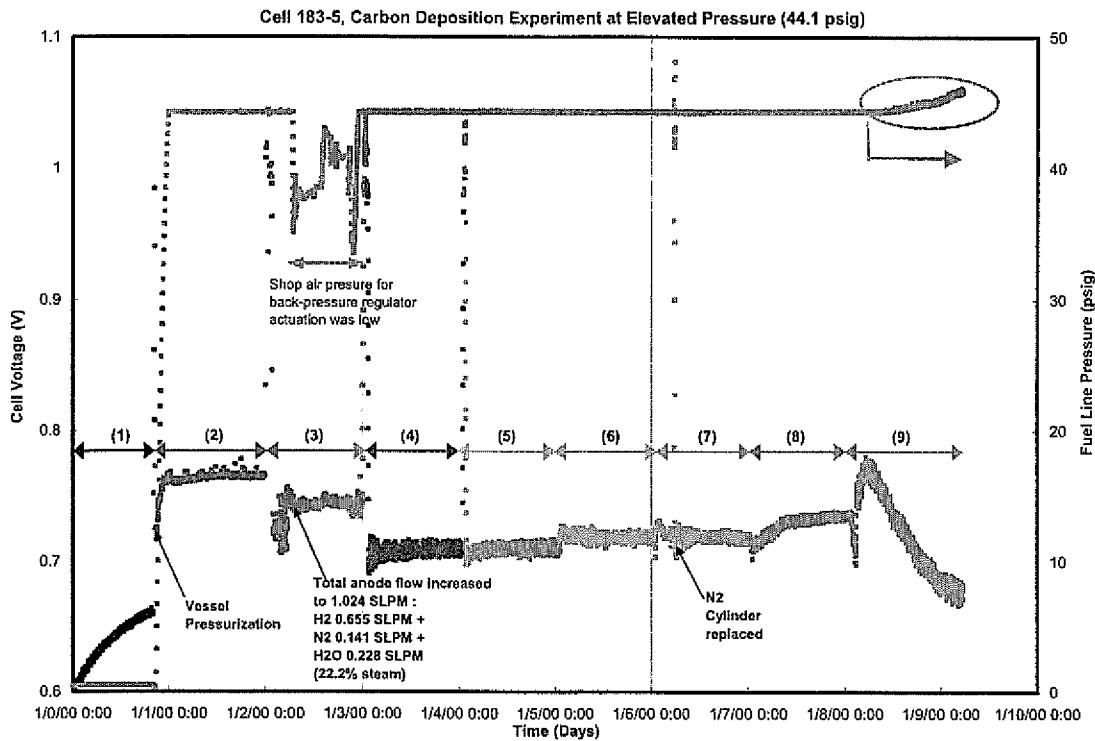
Figure 7: Carbon deposition experiment result at 44.1 psig pressure (numbers in parentheses refer to flow conditions detailed in Table 3)

Anode Fuel Streams employed in Carbon Deposition Test at Elevated Pressure	Current Density (mA/cm^2)	Fuel Utilization (%)	Carbon Deposition Predicted	
			Open Circuit	Under Load
(1) Cell Conditioning, H_2 0.64 SLPM + N_2 0.36 SLPM	370	29.4		
(2) H_2 0.51 SLPM + N_2 0.29 SLPM	286	28.6		
(3) H_2 0.51 SLPM + N_2 0.11 SLPM + H_2O 0.177 SLPM	286	28.6		
(4) S/C 2.0 + N_2 0.363 SLPM,	286	28.6	NO	NO
(5) S/C 1.0 + N_2 0.598 SLPM	286	28.6	NO	NO
(6) S/C 0.7 + N_2 0.672 SLPM	286	28.6	NO	NO
(7) S/C 0.5 + N_2 0.723 SLPM	286	28.6	YES	NO
(8) S/C 0.3 + N_2 0.777 SLPM	286	28.6	YES	NO
(9) (S/C 0.5)x2.2 + N_2 0.362 SLPM	286	13.0	YES	NO

Table 3: Details of flow conditions used in pressurized carbon deposition experiment (see Figure 7)

The vessel was pressurized while the cell was operating on a hydrogen/nitrogen fuel stream. The anode fuel flow rate was maintained at 28.6% fuel utilization at 286mA/cm^2 current density. Pressurization of the vessel from 0 psig to 44.1 psig raised cell voltage from 0.713V to 0.764V.

After 24 hours of stable cell operation at these conditions, steam injection was initiated to understand the effect of steam on cell performance and stability at pressurized conditions. Liquid water flow rate was controlled to achieve 22.2% steam content by

11

replacing part of the nitrogen flow in the anode fuel stream. The 22.2% steam content was the same as that of S/C 1.0 in Table 1 and considered the representative steam content. A fluctuation in cell voltage (±15mV) was observed for the same reasons discussed above. The total anode flow rate was subsequently increased to 1.024 SLPM without changing the mole percentage of hydrogen, nitrogen, and the steam in the anode fuel stream (64% H2, 13.8% N2 and 22.2% H2O). The flow rate was increased because at high pressures the linear velocity is decreased, making it difficult to achieve local flow uniformity and adequate velocity at the exit to prevent back diffusion. Subsequently, all testing was performed with an anode flow rate of 1.024 SLPM by adding nitrogen as needed, to maintain adequate linear velocity. The increase in total anode flow rate raised cell voltage by 0.015V (from 0.73V to 0.745V) through reduced fuel utilization (from 28.6% to 22%).

After 24 hours of stable cell operation with a wet (22.2% H_2O) hydrogen/nitrogen anode fuel stream, the anode fuel stream was transitioned to a S/C 2.0 reformate stream. The cell voltage remained stable at approximately 0.705V for 24 hours of operation and showed no measurable sign of cell voltage degradation. Cell operation was continued by transitioning the anode fuel stream to lower S/C ratios (S/C 1.0, S/C 0.7, S/C 0.5 and S/C 0.3), as shown in Figure 7, for 24 hours each and after confirming stable cell operation at each S/C setting. The cell logged a total of 120 hours of operation.

Followed by the stable cell operation on S/C 0.3 reformate stream, the anode fuel stream was transitioned to S/C 0.5 reformate stream with reduced nitrogen flow rate. To compensate for the reduced nitrogen flow, but maintaining a total anode flow rate of 1.024 SLPM, the S/C 0.5 reformate stream flow rate was raised by 120%, which resulted in a lowered fuel utilization from 28.6% to 13.0%. It should be noted that the reduction of nitrogen flow rate and increase in S/C 0.5 reformate stream flow rate increased the partial pressure of individual reactant gases in the reformate stream. The initial cell voltage measured with S/C 0.5 reformate stream was higher (0.773V) than the preceding S/C 0.5 reformate stream test (0.717V). This higher cell voltage was considered to result from the increased reformate stream flow rate (by 120% compared to the preceding one) and the resultant low fuel utilization (13.0% vs 28.6%).

Once the cell voltage reached 0.773V, then it started to drop at the rate of approximately 4.1mV/hr, indicating carbon deposition. The cell voltage drop was accompanied by a rise in fuel line pressure. The fuel line pressure rise was moderate (less than 2 psi) and was not considered high enough to substantially impact anode flow. Cell operation was terminated under a controlled environment after the cell voltage dropped by approximately 0.1V. The cell module was cooled down under a controlled environment to conserve any carbon deposits that may have been formed.

No carbon deposits was found in the fuel preheating line (upstream of the cell anode). Therefore, it is inferred that the gradual rise in fuel line pressure was the result of carbon deposits accumulating in the anode flow field, as seen in the figure.

SEM-EDX analysis was made on the cell anode to examine the morphology of carbon deposits and the carbon deposit profile across the anode layer. The morphology of carbon deposit over the anode surface was found to be bulky carbon fibers and aggregated spherical carbons (Figure 8).
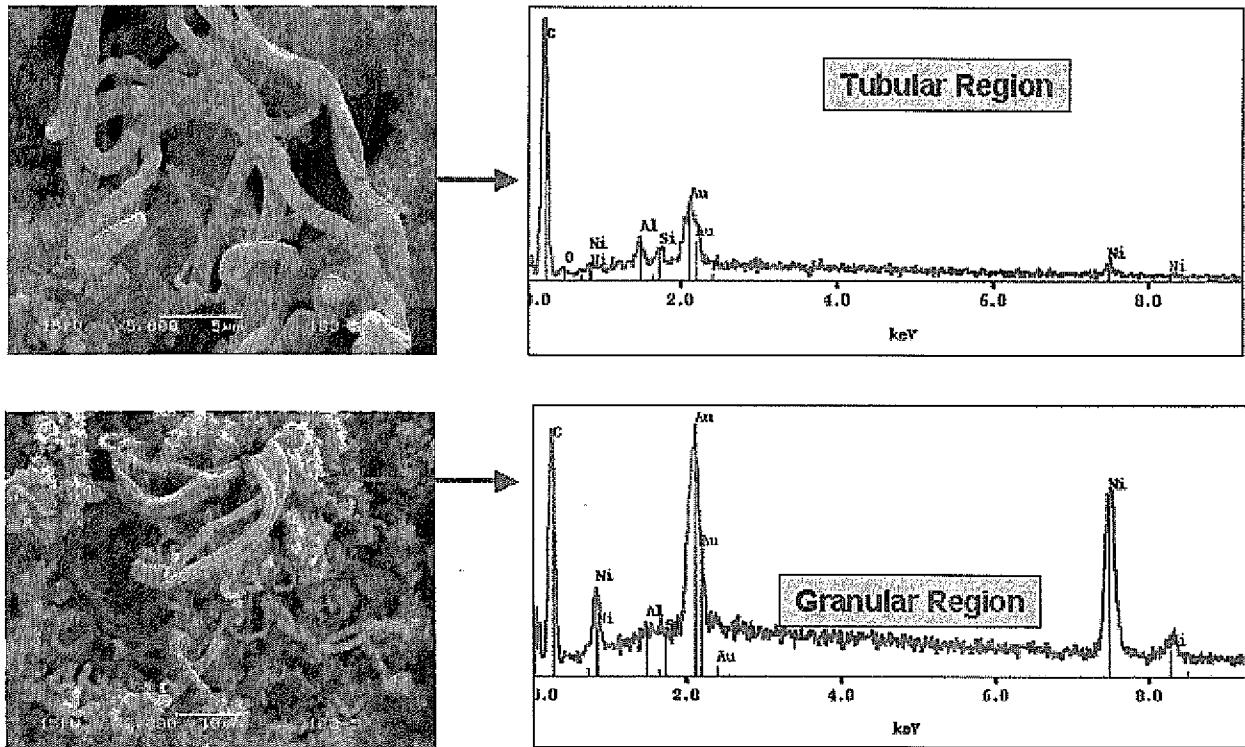

Figure 8: SEM image of carbon deposits over anode surface

The profile of carbon deposit across the anode layer was further investigated to determine whether carbon deposition occurred inside the anode layer. Figure 9 shows an optical microscopic image of the test cell cross-section in the region where carbon deposits were observed over anode surface. Dark black spots were found on certain areas in the active (electrochemical) anode layer. There was very few signs of carbon deposition in the support anode layer.

The profile of carbon deposit was also checked at the electrolyte layer, active anode layer, and four locations in the support anode layer. Figure 10 shows the locations of this analysis and the SEM-EDX spectra obtained. The C peaks in Figure 10 appear to grow as the location moves toward the electrolyte layer with the active anode layer showing the highest C peak. No noticeable C peak was found on the electrolyte layer. This observation does not support the general understanding that anode inner layer is more enriched with H_2O and less enriched with methane compared to the anode outer layer. It is probable that carbon deposits closer to the anode/gas interface might have

13

been removed through reaction with hydrogen during the cool down period since low hydrogen flow was bled into the nitrogen stream during this period.
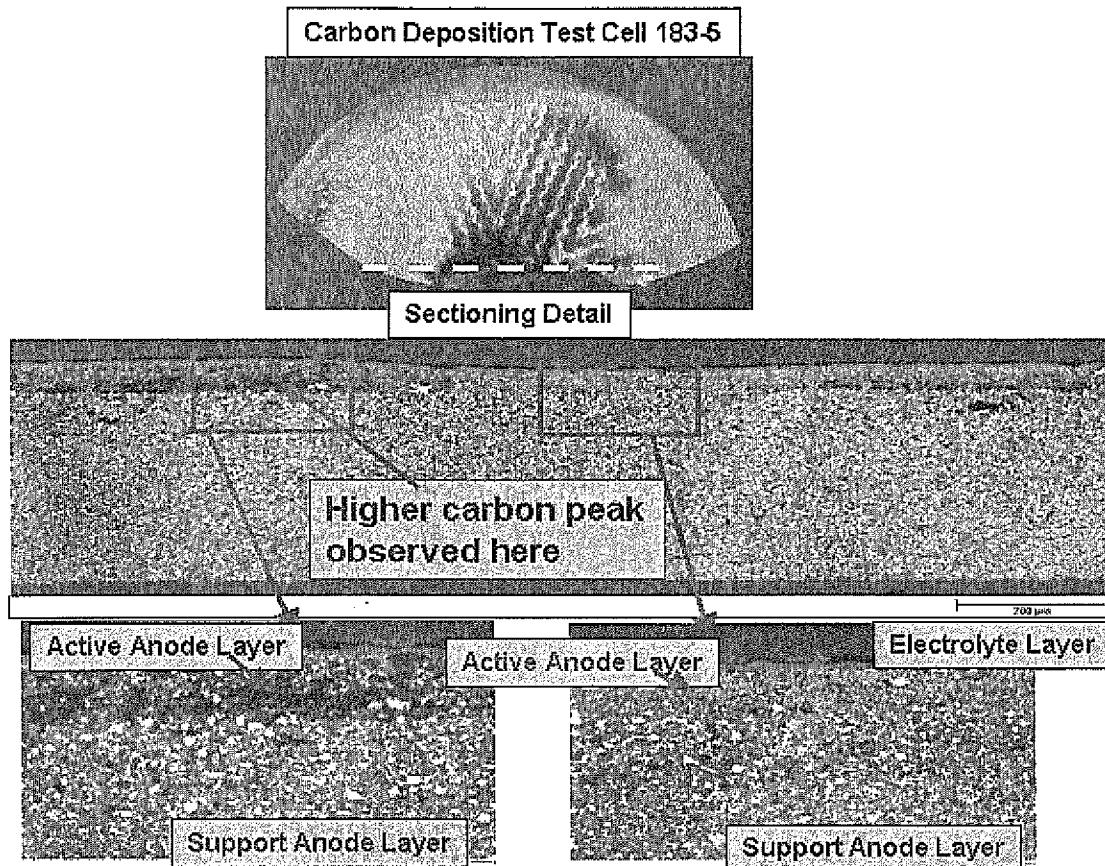
Figure 9: Optical microscopic image of test cell cross-section
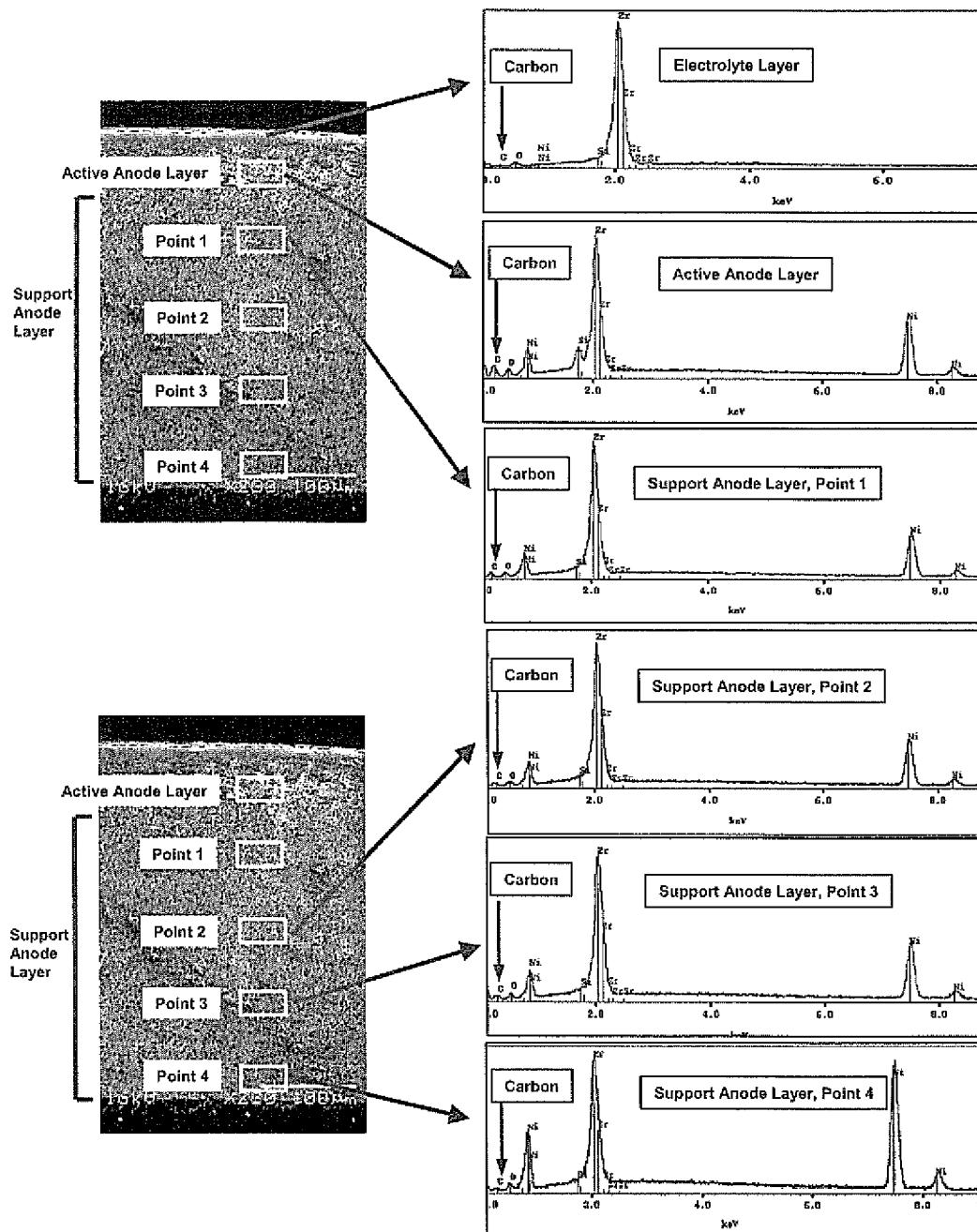
Figure 10: SEM-EDX spectrum across test cell cross-section

1.1.1.4 Discussions and General Conclusions

Along with the ambient and pressurized carbon deposition experiments as shown in Figure 4 and Figure 7, respectively, thermodynamic calculations were performed to understand the operating conditions that are likely to promote carbon deposition in an

15

operating cell. Calculations for ambient pressure operation indicate that S/C 1.0 anode fuel stream in Figure 4 does not deposit carbon under open circuit operating conditions (i.e. with no electric load drawn from the cell) while S/C 0.5 does deposit carbon. When oxygen transfer via current generation from the cell is accounted for, S/C 0.5 anode fuel stream is not predicted to deposit carbon.

Thermodynamic calculations at conditions employed in Figure 7 (elevated pressure) predicts that carbon boundary lies between "(6) S/C 0.7 + N_2 0.672 SLPM" and "(7) S/C 0.5 + N_2 0.723 SLPM" anode fuel streams. Current generation on "(7) S/C 0.5 + N2 0.723 SLPM" anode fuel stream at fuel utilization of 28.6% was shown to add enough oxygen so that no carbon deposition is predicted at the anode outlet region. In Figure 7, cell voltage drop was clearly observed with "(9) (S/C 0.5)x2.2 + N2 0.362 SLPM" anode fuel stream which is also predicted to deposit carbon under open circuit.

In general, the experimental observation of carbon deposition was in line with thermodynamic calculations at open circuit conditions. The higher the steam-to-carbon ratio in anode fuel stream of Table 1 or the higher the O content in C/H/O elemental composition in anode fuel stream of Table 2, the less likely carbon deposition would occur. The experimental results show that cell operation on anode fuel of S/C 1.0 reformate stream (both ambient and pressurized) was stable without any sign of cell voltage drop. This observation suggests that anode fuel compositions corresponding to S/C 1.0 or higher are in a safe operating zone.

Thermodynamically, carbon deposition is favored at pressurized condition. For example, the anode fuel stream composition of S/C 0.7 in Table 1 is predicted to deposit carbon at 3 atm (29.4 psig), but not at 2 atm (14.7 psig). However, its pressure dependence is considered to be very weak and, therefore, the carbon boundary in elemental C/H/O diagram of Figure 1 may not be moved significantly with pressurization. In a working cell, kinetic parameters (such as mass transfer, rate constants, etc) also play important roles along with thermodynamic driving force toward carbon deposition. All these factors are reflected in experimental observations and the contribution of individual factors would be gained more clearly through extensive work over wide ranges of experimental conditions.

1.1.2 Life Test

1.1.2.1 Task Objectives

The objective of this task is to determine the impact of pressurized operation on the SOFC performance stability. Prior to this task, most of the SOFC development and evaluation has been focused on ambient conditions and no long-term data was available on planar SOFC's operated at elevated pressures. The goal is to characterize the SOFC performance stability under pressurized operation in comparison to that of ambient pressure operation and provide guidance for future improvement of SOFC materials and designs, if the performance degradation behaves differently.

1.1.2.2 General Approaches

In the early stages of this program, due to limitations in available test stands, SOFC performance had been evaluated at 2 atm with 3-inch cells. The preliminary data indicated that SOFC performance appeared to decay faster than that under ambient conditions. In this reporting period, several long-term tests were completed. Most of the tests used 4 3/8-inch circular cells with radial sealess design and were conducted at nominal 800°C with 64%H_2/36%N_2 as fuel and air as oxidant. These cells consisted of YSZ electrolyte separating Ni/YSZ anode and LSM/YSZ cathode. Commercially available ferritic alloy was used as interconnect. To reduce interference of fuel utilization, these tests were conducted under moderate fuel utilization (~40%). During tests, the cells were operated under a given current density and pressure, and the cell voltage was monitored over the testing period to evaluate its performance. Cell area specific resistance (ASR) was also estimated from the cell open circuit voltage, operating voltage, and current density. In some tests, AC impedance was also taken before and after the test to evaluate the change in cell impedance. Post test analysis was conducted to characterize the cell microstructure, oxide scale on metallic interconnect, and chromium contamination to electrodes.

1.1.2.3 Fuel Cell Test Results

Figure 11 shows the performance (cell voltage and ASR) of Cell 122 as a function of time under test conditions. After cell reduction and initial polarization, the cell was held at 0.435A/cm^2 and 1atm (ambient pressure). The cell performance continued rising in the first 200 hours and it appeared to be steady between 300-500 hours. The initial performance increase with time is typical for these cells. However, it appears to take longer for the performance to stabilize or start to decay. This process has not been well understood and it is often referred to as "conditioning" of the cell, especially the electrodes. Since the "conditioning" process was long, a higher current density (0.473 vs 0.435 A/cm^2) was used to accelerate the process. However, the cell performance started to decay rapidly, even when the cell returned to the original current density (0.435 A/cm^2).

Nevertheless, the cell module was pressurized to 4 atm and held at 0.435 A/cm^2 for further testing. Again, the cell decayed and the degradation rate appeared to be much faster (voltage loss of ~170 mV within 20 hours) than that at 0.435 A/cm^2 and ambient pressure. Afterward, the cell performance could not be sustained at a lower current density (0.323 A/cm^2). At this point, the cell test was terminated. It seemed that the cell was damaged during the current transition period even though the exact causes remained unclear.

Cell 122, 40% Fuel Utilization
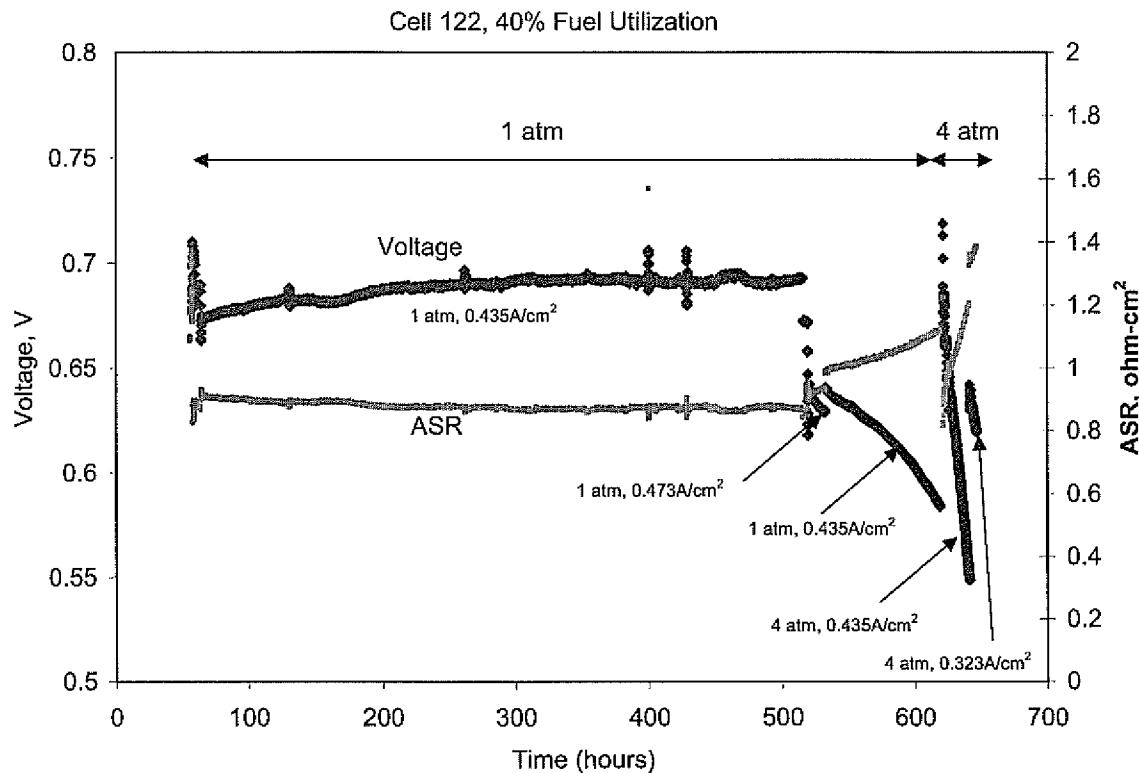
Figure 11: Performance of cell 122 at 800°C with 64% hydrogen balance nitrogen

In parallel to Cell 122, Cell 110 was also tested with the same objective. Figure 12 shows the performance with time of Cell 110. Similar to the Cell 122, the performance of Cell 110 improved over time in the first 640 hours, showing the cell voltage increase and ASR decrease under a fixed current density of $0.3A/cm^2$. After approximately 650 hours, the cell was pressurized to 4 atm and held at current density of $0.379A/cm^2$ for about 100 hours before the furnace malfunctioned. The furnace cooled down unexpectedly while the electronic load continued to draw current from the cell, which damaged the cell. In the approximately 100 hours testing period under 4 atm, the cell voltage appeared steady or slightly decreased in comparison to that observed at ambient pressure (Figure 13).

Cell 110, 40% Fuel Utilization
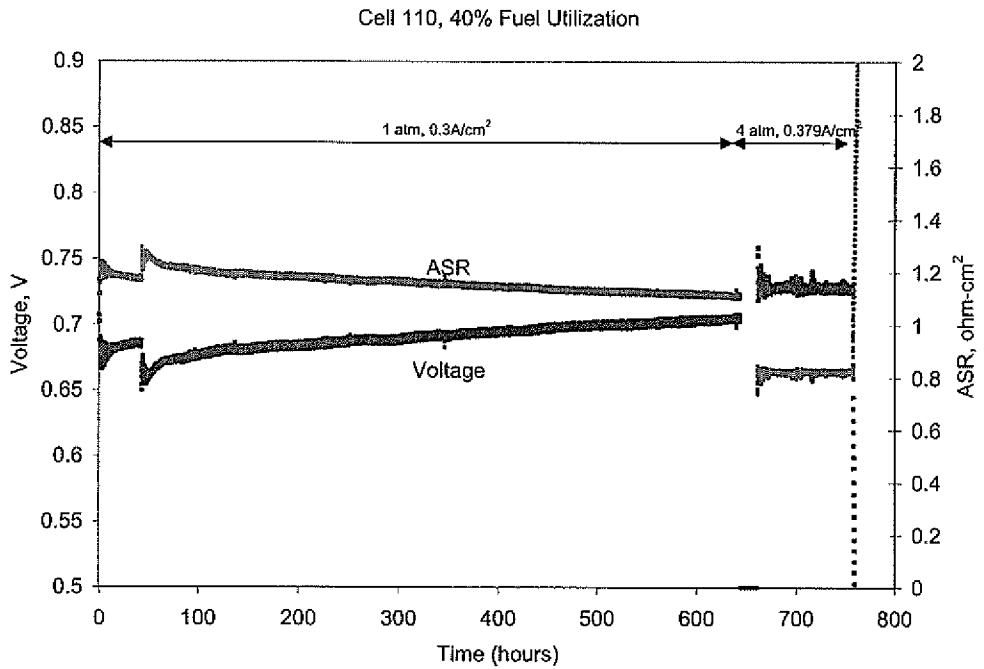
Figure 12: Performance of cell 110 at 800°C

Cell 110, 40% Fuel Utilization
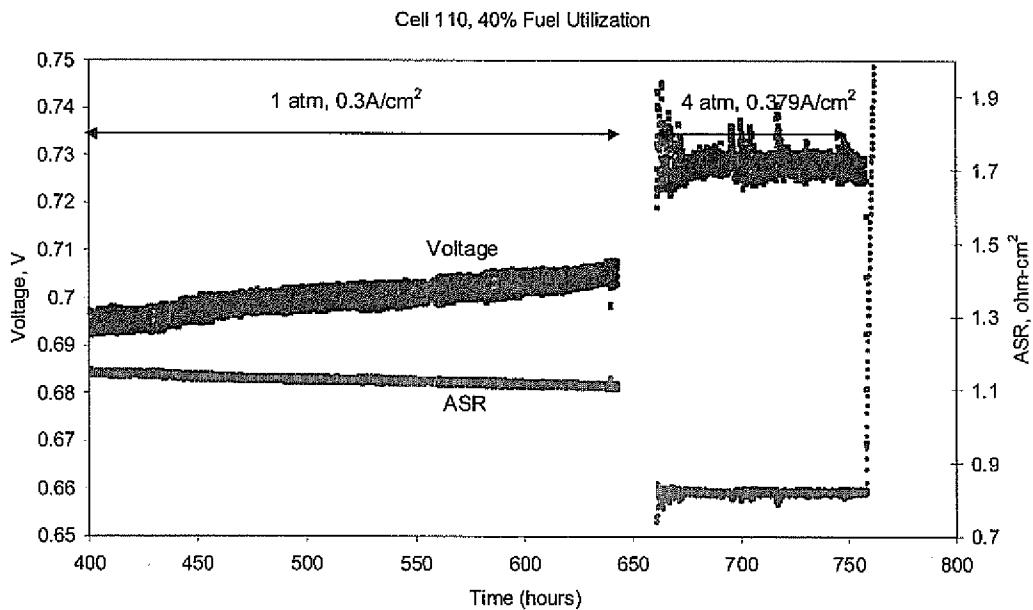
Figure 13: Performance data of cell 110 showing the transit between ambient pressure and pressurized conditions

Since the module performance increased with time in the initial testing period and this conditioning process under ambient pressure was relatively slow as indicated in Cell 110 and Cell 122 tests, a test plan was devised to obtain the performance stability trend under the pressurized conditions first and then switch to ambient conditions. Figure 14 shows the test history of Cell 104. It starts with a 4 atm hold, followed by several steps: at 1 atm, 4 atm, 3 atm, 1 atm and then back at 4 atm. The total duration of this test is more than 1000 hours. In the late stage of this test (from ~900 hours), the pressure fluctuated as much as 5 psi due to a malfunction of the back pressure controller.

During the whole testing period, the voltage appeared somewhat noisy. Despite this noise, the data clearly shows that pressure had a significant impact to the cell performance stability. Cell performance decayed under pressurized conditions in comparison to cell performance improvement (or "conditioning") at 1 atm in the testing period. Close examination of the test data and conditions indicated some of voltage fluctuation arose from the temperature fluctuation of the furnace. The error introduced by the temperature fluctuation was corrected with a transfer function of voltage and temperature obtained in the temperature range between 790 and 815°C. The temperature adjusted data is shown in Figure 15.

Cell 104, 40% FU
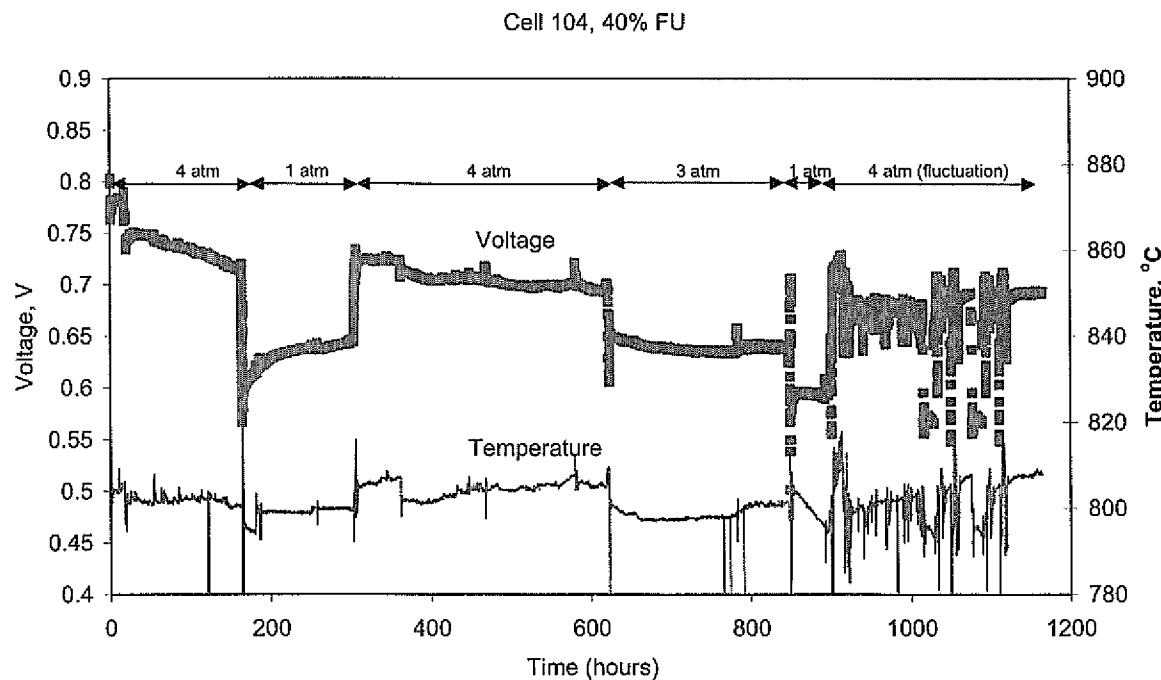
Figure 14: Testing history of cell 104 showing performance and temperature fluctuation
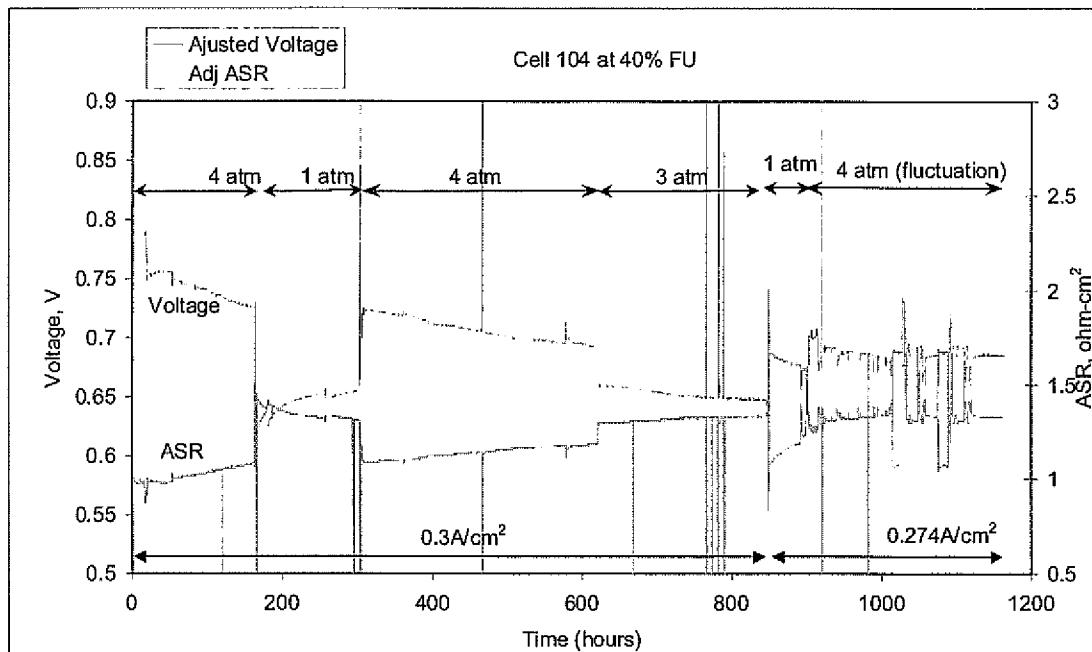
Figure 15: Performance of cell 104 after correction of temperature effect

As shown in Figure 15, the cell voltage decayed under pressurized conditions while the cell performance increased with time once it was switched back to ambient pressure. These results clearly demonstrate the pressure impact to the cell performance stability with time. Based on the data shown in Figure 15, the cell ASR (which includes both ohmic and non-ohmic losses) increased by ~350 mohm-cm^2 after being tested for about 1165 hours.

The AC impedance was also measured on Cell 104 under open circuit conditions at ambient pressure before and after the test. The impedance data (Figure 16) indicates that ohmic resistance of the module increased by ~182 mohm-cm^2 (from ~274 mohm-cm^2 at the beginning of the test to ~456 mohm-cm^2 at the end of the test after 1165 hours). This ohmic resistance increase is about half of the total ASR increase (~350 mohm-cm^2) observed in the performance evaluation.

The impedance analysis also shows that the electrode polarization increases. While the electrode polarization can be estimated from the impedance analysis in principle, the data shown in Figure 16 can only be used as reference because it represents the conditions under open circuit voltage (OCV) at ambient pressure. Due to instrument limitations, AC impedance could not be carried out with current load.
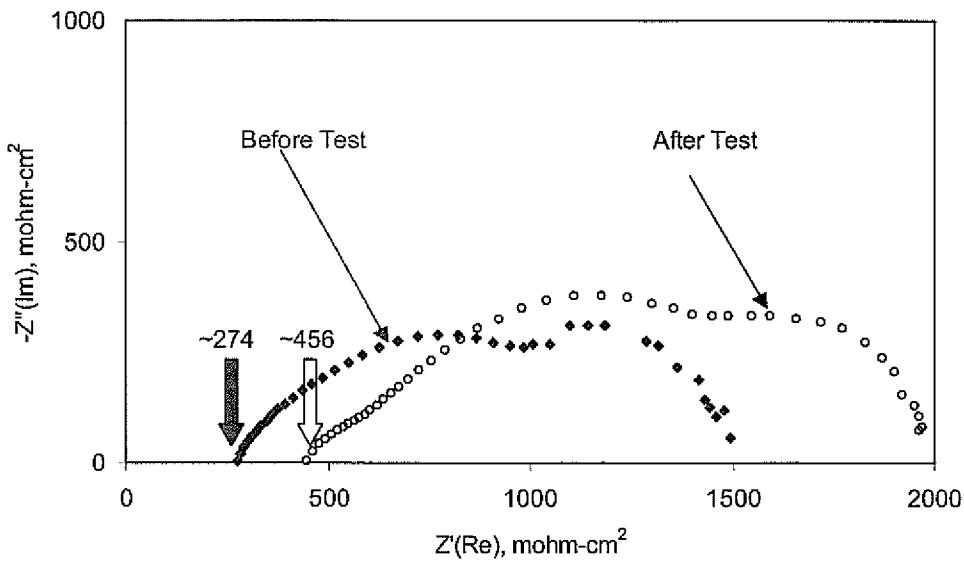
Figure 16: AC impedance taken at 800°C under OCV before and after test

1.1.2.4 Post Test Analysis

Post-test analysis on Cell 104 (Figure 17) did not reveal micro structural anomalies in the cell cathode, electrolyte, and anode in comparison to the cells tested under ambient pressure. The oxide scale was about 2 micron thick, for both the cathode and anode side interconnect (Figure 18). The oxide thickness is similar to those cells tested at ambient pressure for a comparable duration. Silicon-containing material was also detected under the chromium-rich oxide scale. The silicon is believed to be an impurity in the interconnect metal.
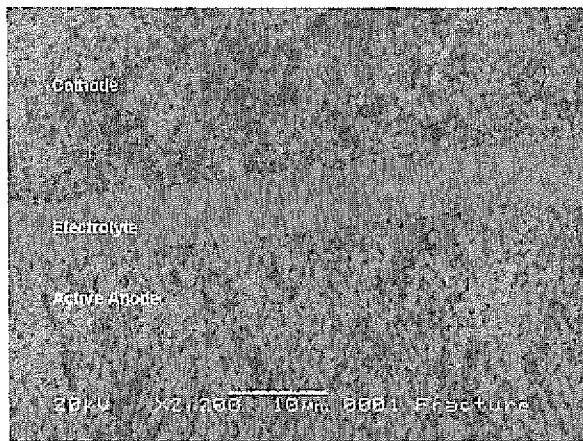
Figure 17: Fracture surface of cell 104 after being tested for more than 1000 hours under pressure
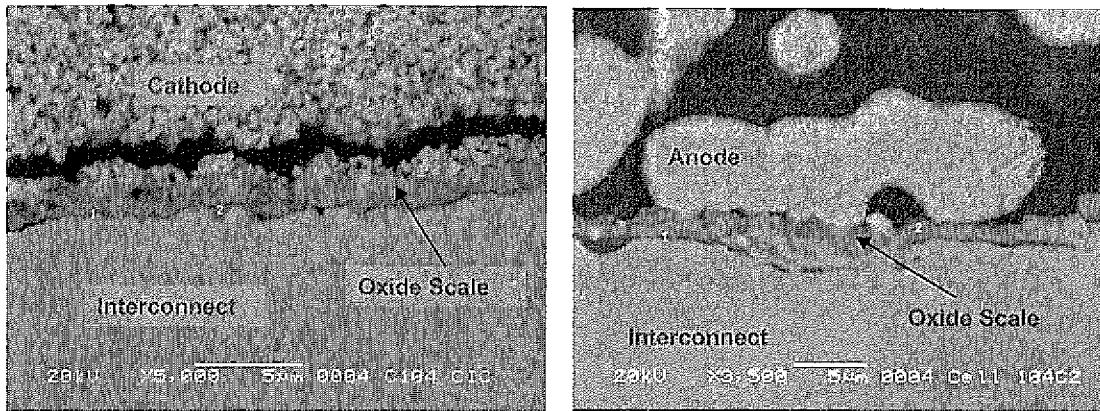
Figure 18: Cross-sections of cell 104 showing oxide growth at both cathode and anode side interconnect

Using an EDX line scan, Chromium was detected between the LSM/YSZ cathode and the metallic interconnect. A slight chromium pile up at the electrolyte/cathode interface was also noticed in the analysis. It appears that the chromium species of metallic interconnect transported and interacted with the cathode materials.

Detailed composition analysis was also conducted on Cell RJ019, which was tested for about 1000 hours. Most of the test time of this cell was at 2 atm pressure. Electron probe micro-analysis (EPMA) was performed in the areas under the interconnect fin (direct current path) as well as the areas open to the gas channel. There are several interesting observations from this data:

- The local chromium pileup at the cathode/electrolyte is clearly seen. In the center and middle portions of the cells, ~1.5-1.6% Cr is observed at the cathode/electrolyte interface. Lower Cr (~0.5%) is present in the edge areas of the cell.

- Chromium presence in a majority of the cathode is low except at the two interface areas.

- Higher chromium (3-5%) is present in the cathode

The profile looks similar to that under the fin area with two exceptions:

- Chromium presence is lower in the gas channel area compared to the area under fin

- At the cathode/electrolyte interfaces, Cr is less than 0.7% and there is little difference from cell center to edge

It is reasonable to believe that the local current densities are higher under the fin areas than the neighboring areas under the gas channels. Since both fuel and air flow is radial from the center to the edge, current density at the center is likely to be higher than that at the edge because of the fuel concentration difference (assuming the temperature

23

is similar). In conjunction with the chromium profile observation, it seems that the Cr transport and interaction with cathode materials may be current related. The higher current density may favor Cr deposition.

1.1.2.5 Hypothesis on Degradation Mechanisms

Major potential causes to cell performance decay include oxidation of metal interconnect, Cr poisoning to electrodes, interface resistance increase, electrode microstructure changes, back diffusion/leakage, and/or electrode conditioning process.

For oxide growth, the parabolic kinetics gives

$$x^2 = k_p t$$

$$or$$

$$x = k_p^{0.5} t^{0.5}$$

where x is the thickness of the oxide scale, k_p is the parabolic rate constant (thickness based) and t is the oxidation time.

For Cr-containing ferritic alloys, the parabolic rate constant depends on the self-diffusion coefficient of Cr and self-diffusion of oxygen. It has been found that the Cr outward diffusion to the oxide scale surface dominates the oxidation kinetics. At a given elevated temperature, the oxygen partial pressure, P_{O_2} dependence of the parabolic rate constant k_p can be estimated with diffusion coefficient of Cr ion in Cr_2O_3

$$k_p \propto D_{Cr} \propto P_{O_2}^{3/16}$$

Thus, the oxide growth thickness based on parabolic kinetics can be estimated as

$$x \propto P_{O_2}^{3/32} t^{0.5}$$

Assuming this relationship is valid for the testing conditions, the thickness of oxide scale in oxidizing environment is expected to increase by approximately 7%, 11%, 14% when pressure increases from 1 to 2, 3, and 4 atm, respectively. As indicated in Figure 18, the oxide scale was about 2 micron after 1165-hour test, which is not much different from those samples tested for similar duration under ambient pressure. It is inconclusive on whether or not the oxide scale grows faster under higher pressures due to the following reasons:

- The resolution is low for moderate growth rate increase under pressures tested, based on parabolic kinetics and the thickness measurements

- The thickness of the oxide scale observed is not representative since the oxide layer can also react with oxygen and water vapor to form vapor species

Another possible degradation mechanism is the chromium poisoning of the cathode, as observed in post-test analysis. This could be electrochemical reaction driven and/or chemical reaction driven. Considering chromium oxide and vapor formation reactions:

- $2Cr (s) + 3/2 O_2 (g) = Cr_2O_3 (s)$ (1)

24
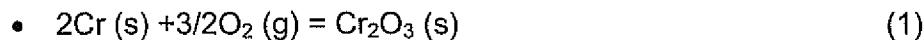
- Cr_2O_3 (s) + 3/2O_2 (g) =2CrO3 (g)   (2) or

- Cr_2O_3 (s) + 3/2O_2 (g) +2H_2O(g) =2$CrO_2(OH)_2$(g)   (3)

Reaction 1 describes the chromium oxide scale formation on Cr-containing ferritic alloys, which will increase the oxide scale thickness as described with parabolic oxidation kinetics. Reaction 2 and 3 describe the possible chromium vapor formation, which could poison the cathode. Under the test conditions, the most possible chromium species may be chromium oxyhydroxide from reaction 3 because of the inevitable presence of H_2O impurity in the air used. The exact mechanism of the chromium contamination through chromium vapor species is unclear at this stage. However, higher operating pressure favors higher chromium-species pressures. Thus, the driving force for chromium vapor species diffusion and subsequent reaction with active cathode materials will be higher under higher pressure.

Other possible degradation mechanisms could also come in play, such as interface resistance increase, electrode microstructure changes, back diffusion/leakage, and/or electrode conditioning process. Exploration of those reaction mechanisms is beyond the scope of this task.

1.1.2.6 Summary

In summary, a number of SOFC module tests have been completed to evaluate the pressure impact to performance stability. The results clearly demonstrate that the operating pressure accelerates the performance degradation. The potential causes to the performance decay include oxidation of the metal interconnect, chromium poisoning to electrodes, interface resistance increase, electrode microstructure changes, back diffusion/leakage, and/or electrode conditioning process. The dominant degradation mechanisms remain unclear. However, current density appears to have an enhanced effect on chromium interaction with cathode material. Both interconnect oxidation and Cr transport to cathode were evident based on post-test analysis. To reduce the degradation related to metallic interconnect, interconnect materials have to be improved or protected with a coating. Future work is needed to understand the degradation mechanisms and the impact of pressure on the electrode conditioning processes.

2   TASK 2.3 – SOFC SCALE-UP FOR HYBRID AND FUEL CELL SYSTEMS

2.1   Scope and Objective

The objective of this analysis is to develop scale-up strategies for large Solid Oxide Fuel Cell (SOFC) - gas turbine hybrid systems (greater than 20 MW) and central station power generation applications. The aim is also to understand effects of system and stack architecture on scaling and performance of multi-megawatt SOFC/GT hybrid systems. System architecture has a significant impact on the design of the SOFC stack and consequently, on the scalability and modularity of SOFC stacks and hybrid systems. Hybrid system concepts with and without recycle (sealed vs. seal-less stack), with and without internal reforming, and with and without stack pressurization are being

considered. Further into the program the optimum practical cell size and building block size will be determined based on plant performance, cost, and reliability.

Analysis will also be performed to ascertain whether a common stack building block can be identified that is suitable for scale-up of power plants of various sizes. Key trade-offs will be explored including reliability, performance, and cost. Consideration will be given to whether the modular building block should extend beyond the stack to include balance-of-plant components or subsystems. The power plant size ranges over which a common modular building block can be expected to be reasonable and the stack and balance-of-plant components contained in the building block will be reported. The largest power plant scale that could appropriately (based upon cost, reliability, and performance) use this building block (sized for a 20 MW system) will be estimated. Stack technology gaps will be articulated and a top-level scale up and technology development plan will be communicated.

The project approach is product focused. Thus stack and system scalability strategies are driven by end-user (power generation industry) functional requirements and not simply by technology limitations. The project plan is depicted graphically in Figure 19.

Task 1 – Product Requirements					
TASK 2 Brainstorm Concepts	TASK 3 Concept Screening	TASK 4 Stack/System Scalability	TASK 5 System Downselect	TASK 6 Detailed Analyses	TASK 7 Stack Gap Analysis
· Reduce Stack Complexity · 55-75% Sys. Efficiency · < $400/kW	· Thermo. Analysis · Downselect Concepts	· Reliability Anal. · First Cost Anal. · Modular Subsys Analysis · Concept Sys. Scalability > 20MWe	· Cost, Reliab., Perf. vs Functional Spec. · Downsel. Single Concept Sys.	· Refined Perf. · Refined Cost · Refined Reliability · Optimize Sys. · Define Module · Scale-up Strategy	· Systems Top-Down vs Technology Bottoms-up · Proposed Development Program
Task 8 – Program Management and Reporting					

Figure 19: Graphical representation and inter-relation of proposed project tasks

2.2 Product Specification

Current 20 MW power generation systems primarily consist of small gas turbines including aero-derivatives and heavy-duty gas turbines. Aero-derivative turbines are typically used for peaking applications since they provide exceptional dynamics. However, they also command higher prices. Small frame heavy-duty gas turbines are primarily utilized in mechanical drive and combined heat and power applications. In general, solutions in the 20 MW size range are operated in cyclic or peaking duty.

SOFC hybrid product attributes and customer economics dictate that SOFC hybrid systems provide the best customer value at base load. Consequently, it is not appropriate to derive the product specifications of the SOFC hybrid system based on the specifications of current 20 MW systems that are operated on cyclic or peaking duty.

Despite its higher power rating, GE's 7 FB-gas turbine in a combined cycle plant has the closest product requirements, providing 275 MW power at base-loaded operation as

26

well as highly competitive cost of electricity for supplying power to the grid. The product specification of the GE 7 FB-gas turbine was therefore used as a basis for the product specification developed for the SOFC scale-up task. The requirements of the solicitation of work for the SOFC scale-up task were also incorporated into the function product specification. The design target for the power generation system in this task is 25 MW. Attributes particularly important to this project include reliability, efficiency, first cost, and cost of electricity.

2.3   System Concept Brainstorming

In a SOFC system, the air stream has to satisfy two conflicting requirements: it has to heat the cell to its operating temperature and at the same time, provide a convective cooling mechanism so that the cell does not overheat. Additionally, in a hybrid SOFC system, the enthalpy the air stream absorbs inside the stack is used in the expander to do useful work. Thus the stack entry and exit temperatures as well as the air mass flow rate play a key role in the system performance. These considerations make the air stream management one of the most important aspects of SOFC system design. Specifically, the means to raise the compressor exhaust air temperature to the desired SOFC stack inlet condition, the management of the stack exhaust air, and the enthalpy addition in the stack itself require particular attention in the design of the system. The enthalpy addition in the stack depends on the stack design and operation, while the first two are important aspects of the system design.

Several other issues must also be addressed during system design. First, the enthalpy of reaction that must be supplied to the reforming reactor could either be thermally neutral, or be positioned where excess heat is available. Second, the unutilized fuel from the stack must be consumed. Since this fuel contains carbon monoxide, there is a potential safety and environmental concern in addition to the plant efficiency concerns. Finally, a large quantity of high quality water is required for natural gas reforming. This water must be supplied to the system or water internal to the system must be used in an efficient way to reduce the requirements.

As one of the primary tasks in this system study, a large number of system and stack concepts were evaluated that address these and other issues. These concepts were drawn from a variety of sources, including those published in literature.

All the brainstormed concepts were subjected to the use of a Six Sigma tool, the Pugh Matrix, for ranking based on projected system efficiency, cost and reliability. Engineering judgment, rather than quantitative analysis was used to reduce the list of system concepts from twenty-five to four. The four downselected concepts were chosen based on the following characteristics:

- Flexibility: the downselected concepts were flexible enough to generate variants. During the detailed analysis phase, some of the variants may be explored for improved efficiency and reliability or reduced cost.

- Completeness: the concepts incorporated a spectrum of features. For example, the four systems incorporated the trade between sealed and sealless stacks, staged and parallel stacks, recycled and non-recycled systems, etc.

- SOFC stack pressure: the downselected systems may be operated over a wide range of SOFC stack pressures.

2.4 Modeling

Design point performance models were created for each of the four downselected concepts described above. Heat and material balances have been performed using system-level SOFC performance models. The model estimates the system's net power level, SOFC power, turbine power, and the system efficiency. The resulting data at each state point is then linked to the reliability and cost model to estimate the reliability and cost of the power plant.

2.4.1 Performance Modeling

The thermodynamic performance model, when coupled to the stack model allows the overall plant efficiency of the system concept to be estimated as a function of operating assumptions (such as operating pressure). Operating assumptions for the various concepts have been tested and parameterized to assess the potential performance of each plant concept and to ensure that the performance requirements of the subsystems and components are consistent with solid engineering design practice.

The primary assumptions made in the performance analysis are the following:

- All cost and reliability assumptions do not differ between the sealed and the seal-less stacks.

- The maximum air temperature rise through the SOFC stack assembly (sealed and seal-less) is assumed to be100°C.

- The maximum SOFC outlet temperature is assumed to be 775°C. This limitation comes from the maximum allowable metal interconnect temperature.

- The SOFC single-cell voltage at the design point conditions is assumed to be 0.7V.

- The one-pass fuel utilization is assumed to be 70%. One-pass fuel utilization is described below.

- The SOFC subsystem pressure drop is assumed to be a constant 5% of system pressure. The SOFC stack pressure drop is assumed to be no less than 1 psid per stack.

- The power density is assumed to be a function of the SOFC pressure, as shown in Table 4.

Operating Pressure, atma	1	2	3	4	5	6	7	8	9	10	11
Power Density, W/cm2	0.440	0.466	0.482	0.493	0.502	0.509	0.515	0.520	0.525	0.529	0.532

Table 4: Power density as a function of pressure

One-pass fuel utilization is defined as the fuel consumption per pass (from stack inlet to exit) divided by the inlet fuel flow rate. Thus, for a system having recycle, the total fuel utilization is higher than one-pass utilization because part of the fuel is recycled back to the inlet. The relationship between the total utilization (u_t) and the one pass utilization (u_p) is shown below:

$$u_t = \frac{u_p}{1 - r(1 - u_p)},$$

where r is the recycle ratio defined as the amount of recycle flow divided by the stack exit flow. A recycle flow is chosen so that a steam to carbon ratio of 1.5 is obtained. This corresponds to about 50% recycle.

2.4.2 Performance Analysis Results Summary

The results for the downselected four system are summarized in Table 5. The analysis is performed with pressure as a parameter.

29

Concept1					
Pressure (atm)	5	6	7	8	9
Power density (W/cm2)	0.502	0.509	0.515	0.52	0.530
Fuel Cell Power (kW)	20509.69	20342.07	20154.03	20255.27	20314.52
Gas Turbine Power (KW)	6334.753	6291.699	6181.29	6138.074	6082.848
System Power (kW)	25000	25000	25000	25000	25000
Efficiency	64.89	65.43	65.64	65.71	65.53
Concept 2					
Pressure (atm)	6	7	8		
Power density (W/cm2)	0.509	0.515	0.52		
Fuel Cell Power (kW)	18639.12	18627.85	18656.21		
Gas Turbine Power (KW)	7687.112	7632.315	7556.648		
System Power (kW)	25000	25000	25000		
Efficiency	60.59616	60.63253	60.54007		
Concept 3					
Pressure (atm)	4	5	6	7	
Power density (W/cm2)	0.502	0.509	0.515	0.52	
Fuel Cell Power (kW)	19996.28	19810.67	20198.24	20912.33	
Gas Turbine Power (KW)	5476.185	5663.672	5287.994	4600.389	
System Power (kW)	25000	25000	25000	25000	
Efficiency	66.56006	67.1867	65.90245	63.65319	
Concept 4					
Pressure (atm)	4	5	6	7	
Power density (W/cm2)	0.502	0.502	0.509	0.515	
Fuel Cell Power (kW)	20115.88	19959.2	20650.48	21475.99	
Gas Turbine Power (KW)	5155.068	5348.264	4702.583	3923.476	
System Power (kW)	25000	25000	25000	25000	
Efficiency	66.16692	66.68719	64.45835	61.98567	

Table 5: Summary of system concept performance

2.4.3 Reliability Modeling

A reliability analysis tool for the hybrid SOFC plant was developed. The term reliability is generally used to indicate the ability of a system to continue to perform its intended function (IEEE Std 493-1997). The scope of this project does not include a detailed

design-for-reliability task. The purpose of this model is to allow key reliability trade-offs to be made against various stack and system scale-up strategies. For the purpose of evaluating stack scale-up strategies based upon modular building blocks, the developed reliability model that focuses on the stack(s), multi-stack modules and power electronic package(s). This model has been used to demonstrate the impact of various multi-stack/power electronics configurations on the system reliability, the results of which have been incorporated into scale-up strategy and modularity recommendations and subsequent final system down-selection.

The key concepts in defining the system reliability are MTBF (mean time between failure) and MTTR (mean time to repair). The MTBF is defined as the mean exposure time between consecutive failures of a component. The MTTR is defined as the mean time to repair or replace a failed component. Two major assumptions were made to simplify the roll-up of component reliabilities into a system reliability:

- The principal failure mode of each component is considered
- The failure rate is constant over the life of the power plant

MTBF and MTTR for all the system components (except the stack and the reformer) were collected from various published data. MTBF and MTTR for the stack and reformer were collected from expected/projected data published in the literature. At this preliminary level, stack MTBF and MTTR were assumed to be independent of size, utilization and loading.

For a multi-stack power plant, several redundancy strategies were considered. Several stacks make up a module and several modules make the plant. At this preliminary level, redundancy is chosen only at the module level, i.e., the plant consists of N working modules and M redundant modules (M is a small integer, usually less than 3). The redundant modules are in a standby mode. In case of a stack failure, the module containing the failed stack would be isolated, shut down and repaired, while one of the redundant modules will be operated to supply the rated power.

The main studies that will be performed using this tool are:

- Plant Reliability and Availability for a varying number of stacks in the module, number of modules in the plant and the number of redundant modules. Availability is the long–term average fraction of time that a component or system is in service and satisfactorily performing its intended function (definition per IEEE Std 493-1997)

- Effect of component MTBF and MTTR on the plant Reliability and Availability.

2.4.4 Cost Modeling

A first cost model has been developed for each of the four systems concepts. Component cost values have been used to develop full plant first cost estimates. The model is parametric, so the effect of system design on cost could be easily explored. All

31

the component costs are duty based. Thus sensitivity studies like the effect of system pressure, effect of amount of recycle, various levels of internal reforming etc. could be performed. The scope for all the costing is manufactured cost (and not installed cost).

The model could be exercised in several modes. The default configuration is the nominal mode, where all the component costs reflect current market conditions. In the 'entitlement' mode, the best-case scenario costs are used. The component cost data for the nominal mode is drawn from a variety of sources, including vendor quotes, catalog prices for commodity items and projections for special items. For the stack, simple roll-up from nominal raw material prices was assumed. Engineering judgment was exercised in the entitlement mode for the best-case costs, and factors such as 20-yr projections for raw material prices, opportunities for better yields, improvements or changes in technology and bulk pricing are taken into account.

2.5   Concept Analysis and Downselection

A quantitative method for ranking the systems was developed in order to downselect a single concept from the four concepts described earlier. The scoring system is based on the product specification, and formulated to give due importance to cost, reliability, and performance. The following formulation was used for establishing a score for each system:

Score = (efficiency/0.65) + (reliability/0.985) + (MTBF/4380) + (400/cost_per_kW)

For each concept the following steps were undertaken. First the system efficiency was calculated using the performance model. A preliminary bill of materials (BOM) was then established. This BOM was the basis for estimating the system cost, reliability, and MTBF using the cost and reliability models. Subsequently, the system score for each concept was calculated. A summary of the optimized results is shown in Table 6.

Parameter	Concept 1: Sealed Recycle	Concept 2: Seal-less Recycle	Concept 3: Mass Addition	Concept 4: Interstage HX
Optimal Pressure (atm)	9	8	5	5
System Power (kW)	25000	25000	25000	25000
Fuel Cell Power (kW)	20315	18656	19811	19959
Gas Turbine Power (KW)	6083	7557	5664	5348
System Efficiency, %	65.53065	60.54	67.19	66.69
Cost	$23,503,213	$24,370,313	$24,034,415	$23,932,819
Specific Cost, $/kW	$940	$975	$961	$957
Reliability	94.75%	94.75%	94.75%	94.75%
mtbf, hrs	1258	1258	1182	1146
Total Score*	2.6828	2.5909	2.6816	2.6675

Table 6: Analysis results for four concepts at optimum pressures

Concept 2 drops out due to its low efficiency and higher cost. Since seal-less stacks may offer a potential for lower stack development cost it will be considered a risk-mitigation option for stacks having high-temperature seals.   This option will be discussed further in the final report. Seal-less stacks may be considered a near-term

32

system option as well as a system option for programs with lower efficiency requirements.

Efficiency and cost are comparable for concepts 1 and 3. However, concept 3 operates with a varying air mass flows through stacks, resulting in a challenging stack design or non-identical stacks. Therefore, from system operability point of view concept 3 is not desirable and, therefore, it was eliminated.

Concept 4 drops out due to lower reliability and MTBF resulting from the presence of high-temperature heat exchangers. This leaves concept 1 as the downselected concept, selected for further analysis and development.

2.6 Conclusions and Next Steps

Based on the selection criteria and process described above, concept 1 was downselected for further analysis to include further optimization of the system for reliability, cost, and efficiency and the identification of key technology gaps and barriers. Specifically, a detailed flow sheet, refined reliability, cost and performance analysis will be completed for the downselected concept. Sensitivity analysis of key parameters will be performed to establish the key drivers and identify the technology gaps that are to be closed to meet the product specification. In addition, detailed power conditioning topologies will also be studied for the downselect concept.

Concurrently, the reliability and cost models developed will be used to undertake a stack subsystem sizing analysis for each of the four system concepts. Given the stack technology required for each of the four concepts, the reliability and cost models will be used to examine the trade-offs in cost and reliability of the stack subsystem. The results will be parameterized as a function of cell size, number of stacks, and subsystem composition. This analysis will further explore the reliability, performance, and cost trade-offs for the systems considered and will aid in the identification of the optimum SOFC cell size and SOFC module size.

3   TASK 2.4 – STACK HYBRIDIZATION

The objective of this task is to demonstrate operation of planar SOFC stacks and their operating characteristics under hybrid environment and assess scalability of stack design. SECA derived technology will be leveraged in this task. The work will focus on stack testing of various sizes under hybrid conditions, such as temperature, pressure, and gas composition, which are critical to the development of megawatt class hybrid demonstration systems. Stack performance as a function of fuel utilization will be determined. Analysis of design features that influence stack reliability, performance, and scalability (area and height) will be performed. The dynamic performance of stacks under hybrid conditions including startup and shutdown will be evaluated. Designs and operating procedures to facilitate stack scaleup will be identified.

3.1.1 Schedule and Milestones

A kick off meeting for the stack hybridization was held on Monday, June 7, 2004. A detailed schedule and milestones for the entire stack hybridization task was developed during this report period. All top-level tasks such as stack design/risk review, facilities readiness review, stack hybridization tests are included in the detailed schedule.

3.1.2 Stack Definition and Test Conditions

The requirements for pressurized operation of the SOFC stack in hybrid conditions, such as fuel composition, fuel utilization, and stack operation temperature, have been flowed down from system analysis. Even though there is no detailed stack specifications for this task, a 20-cell stack with 142 cm^2 active area per cell is planned to be tested under simulated steam-reforming fuel as the final and overall goal for this task. The performance of the SOFC stack as a function of pressure, temperature, and fuel composition at hybridization conditions will be identified. Three different steam-reforming fuels that simulate the performance variation of a steam reformer will be used in this task. The detailed fuel compositions are listed in Table 7. The setup of two SOFC pressurized test stands have been initiated based on these specifications.

Steam Reforming Fuel, mole fraction	Design Composition	Off Design Composition 1	Off Design Composition 2
H_2	30.00%	27.83%	25.38%
H_2O	27.55%	35.26%	30.23%
N_2	0.00%	0.00%	0.00%
CO_2	19.73%	23.27%	21.49%
CH_4	13.61%	5.36%	16.54%
CO	9.11%	8.28%	6.36%
Total	100.00%	100.00%	100.00%

Table 7: Compositions of simulated steam-reforming fuel

3.1.3 Risk Analysis of Stack Hybridization

A failure modes and effects analysis was performed during the report period to identify the potential failure modes for large stack tests under hybridization conditions. Twenty-nine potential failure modes covering five broad categories (materials, stack design, stack assembly and installation, stack operation under pressurized condition, and design of pressurized test stand) were identified. Recommended actions to mitigate the major risks were also identified.

Activities to evaluate the current SECA stack design for critical and necessary design changes have been initialized. The requisite design changes are expected to be minor and therefore planned to be completed shortly, in preparation for procurement activities.

3.1.4 CFD Analysis for SOFC Stack Flow and Thermal Distribution

The failure modes and effects analysis identified risks associated with the use of a SECA-based stack for pressurized operation. One such risk involves the changes in the gas volumetric flow rate and gas thermal properties that result from pressurized operation. In order to retire this risk the thermal performance of a single cell stack was simulated under pressurized (4 atm) and ambient conditions using a 3D computational fluid dynamics (CFD) model. The model was based on a half-sealed circular configuration with 16 cm cell diameter. The cell temperature difference and the temperature gradients were found to be about the same as that at ambient pressure. Flow distributions for the anode and cathode flow fields were also found to be similar to that at ambient pressure.

Conclusion

The following activities have been carried out during this reporting period. The results from these activities are summarized in this report.

➢ Evaluation of the impact of pressure on the carbon deposition boundary on operational SOFC cells.

➢ Evaluation of the impact of pressure on the performance degradation and cell conditioning of SOFC cells.

➢ Definition of requirements and identification of risks for the demonstration of the operation of SOFC stacks and their operation characterization under hybrid system environment.

➢ System analysis to establish the scale-up strategies for large (greater than 20 MW) SOFC-gas turbine hybrid systems for centralized power generation applications

References

K. Sasaki and Y. Teraoka, Journal of the Electrochemical Society, 150 (7), A885, 2003

EXHIBIT 2

2005 SECA Core Technology Review

Review of Fuel Processing in the SECA Core Program

April 21, 2005

by

David A. Berry
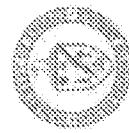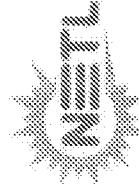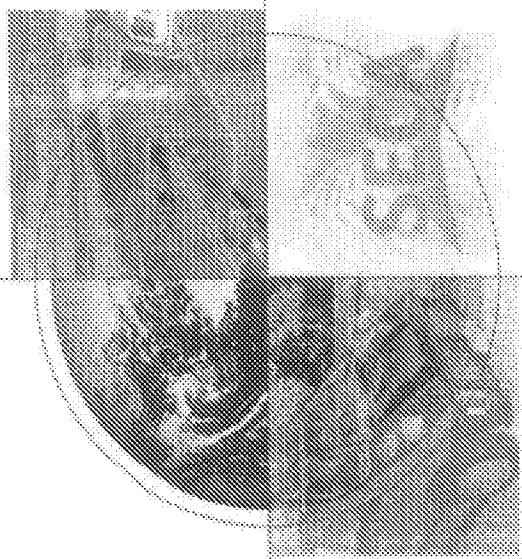
SECA Program Vision:
A Single Mass-Manufactured Core Module

Stationary

Transportation

Military

Core Fuel
Cell Module
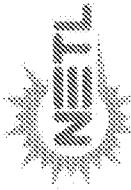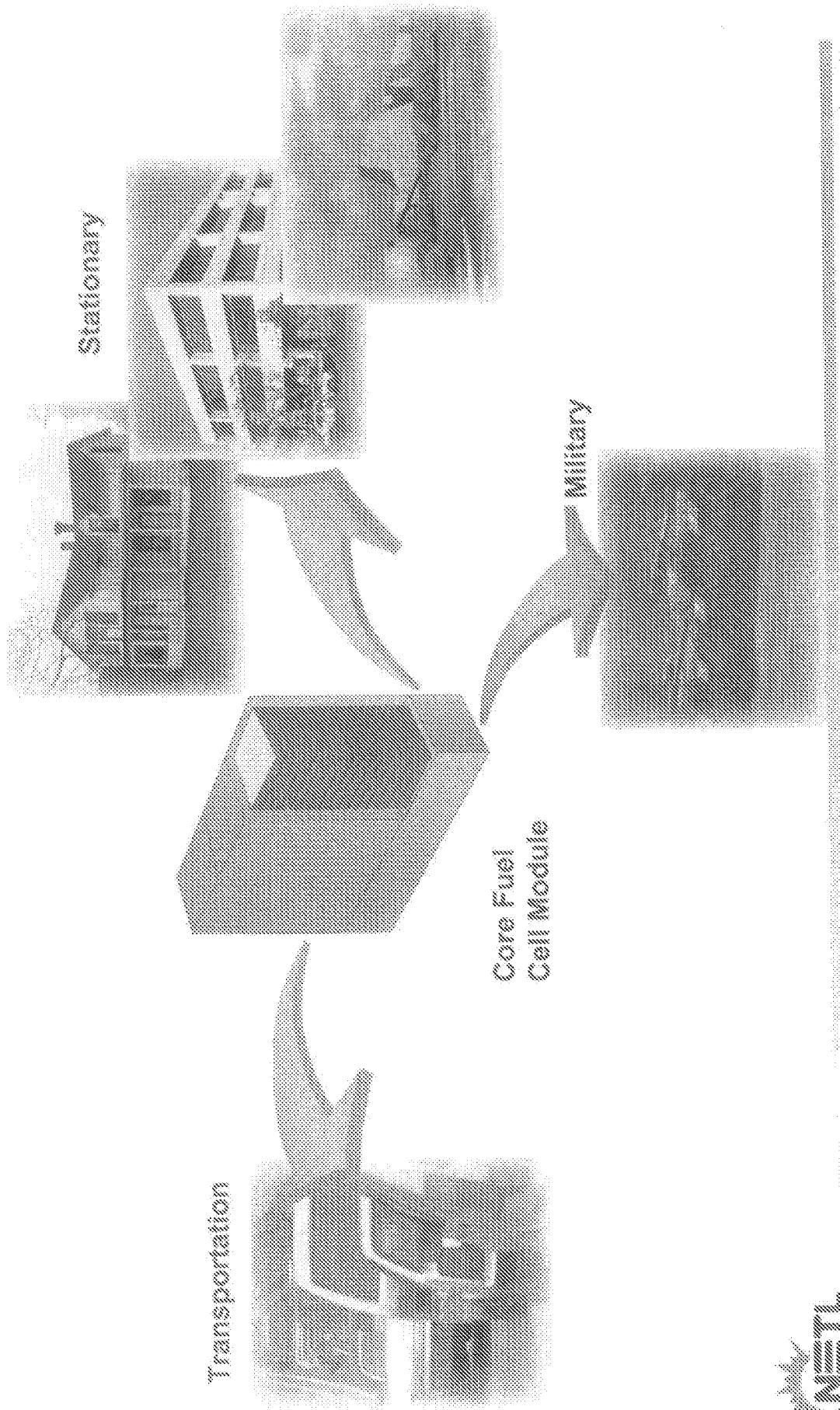
SECA: A Path to Making Fuels Cells a Reality
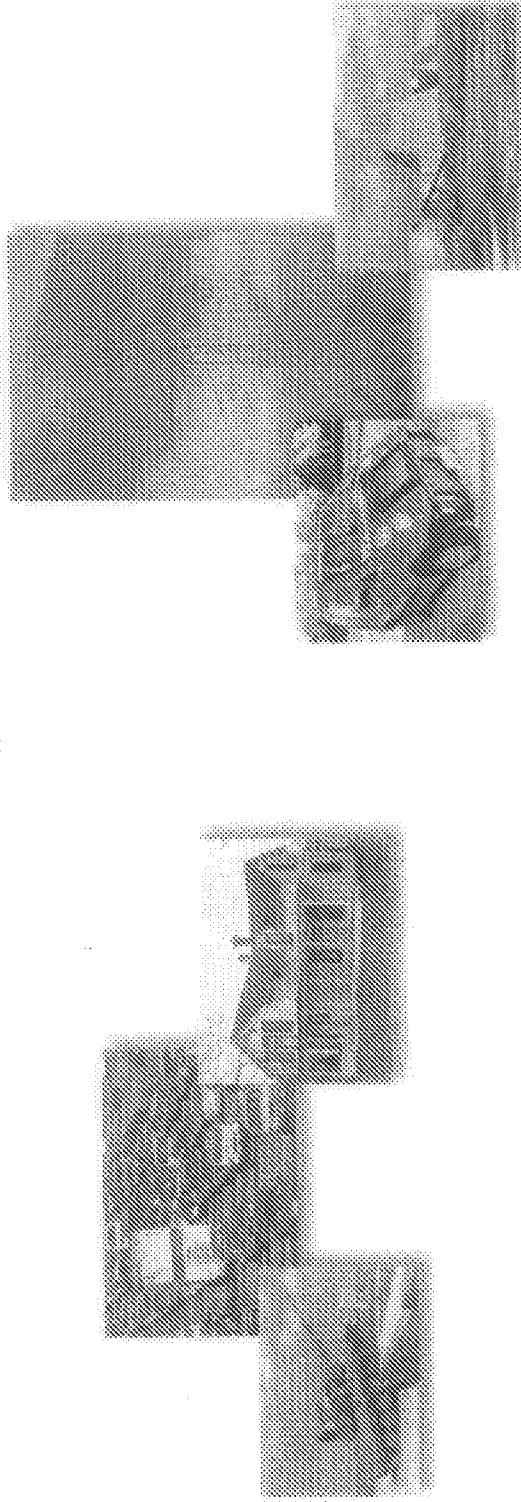
2005

- 1st Generation Prototypes
  - Testing & Evaluation

2010

- **$400/KW Modules**
- Commercial products
  - Residential, Commercial, Industrial CHP
  - Transportation APUs

2012 - 2015

- Hybrid Testing at FutureGen

2020

- MW-Scale Hybrids for Advanced Coal Power Plants

NETL

SECA Industrial Teams

General Electric Company

GE Power Generation

DELPHI

Acumentrics
Advanced Power & Energy Technologies

FuelCell Energy

SIEMENS
Westinghouse

NETL
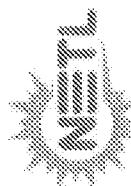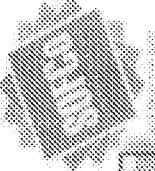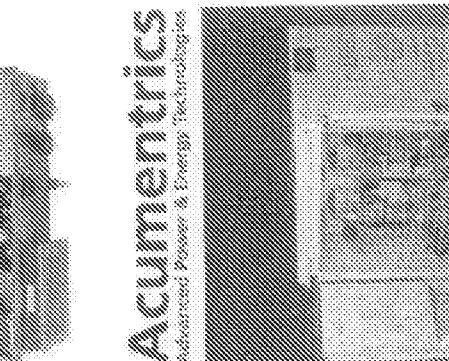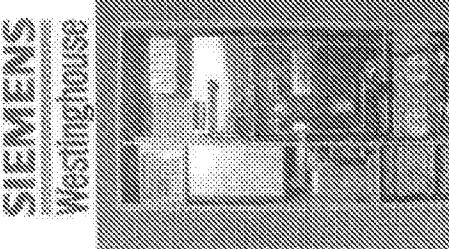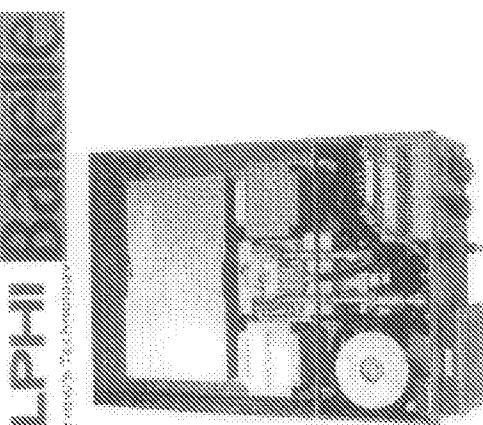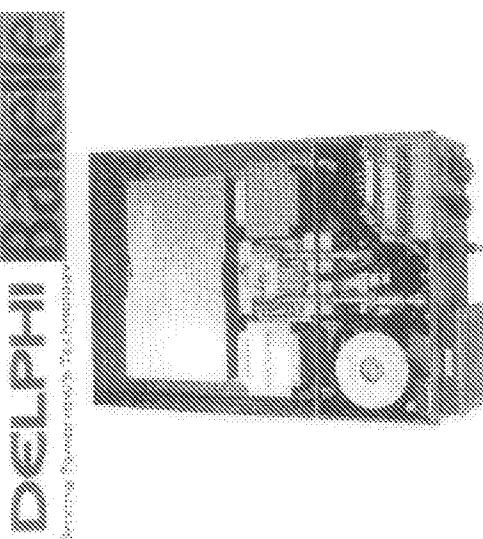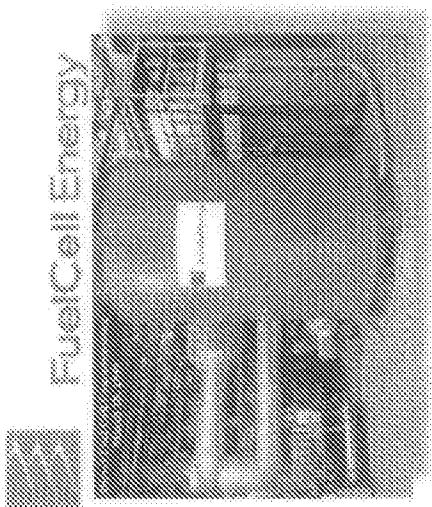
Fuel Processing for SECA

Commercial fuels – A variety of development issues

Sulfur
poisoning

Coke
formation

High efficiency &
thermal integration

Quick startup and
transient response
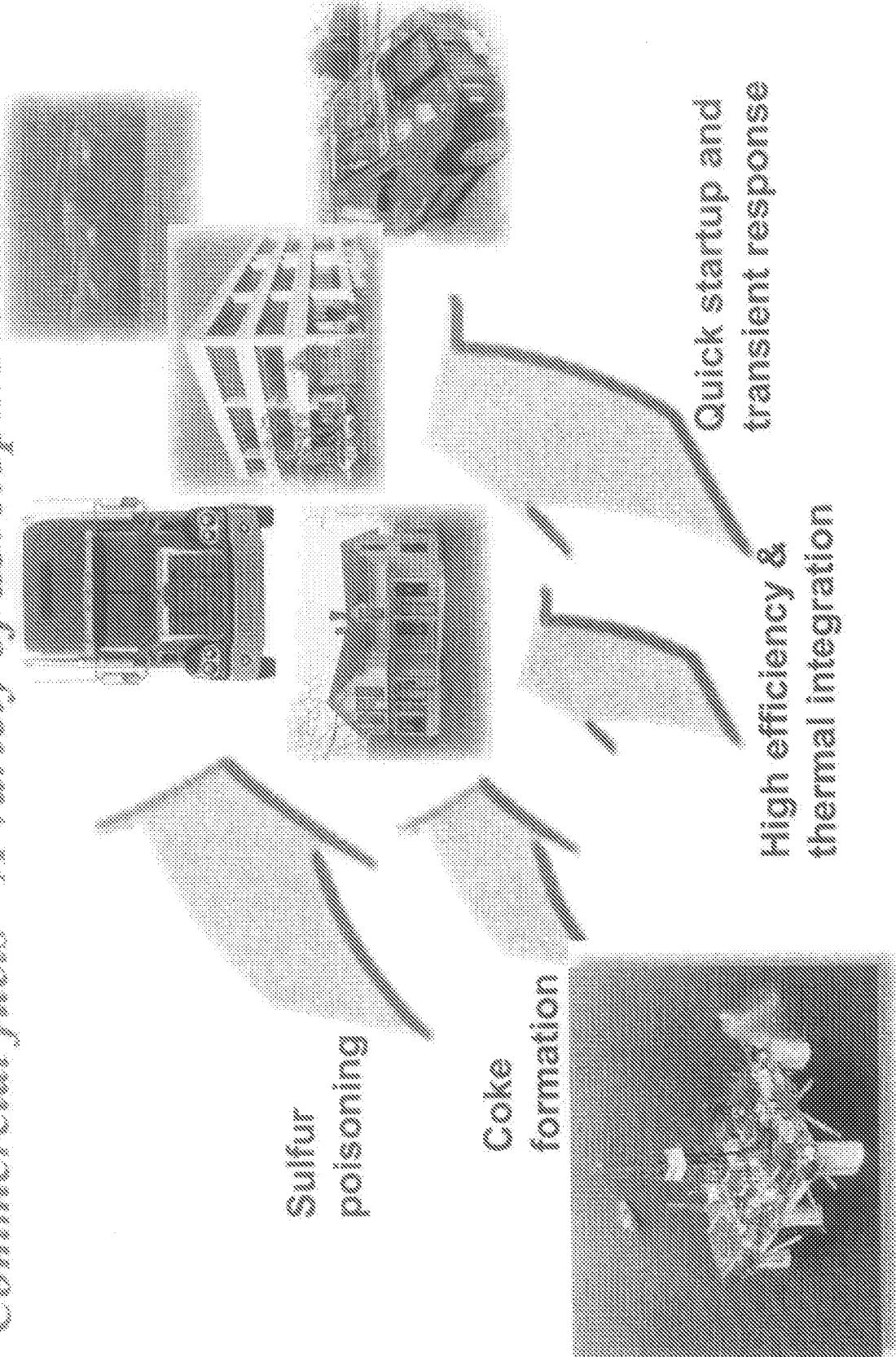
Fuel Processing Focus Area
Technical Issues / Challenges
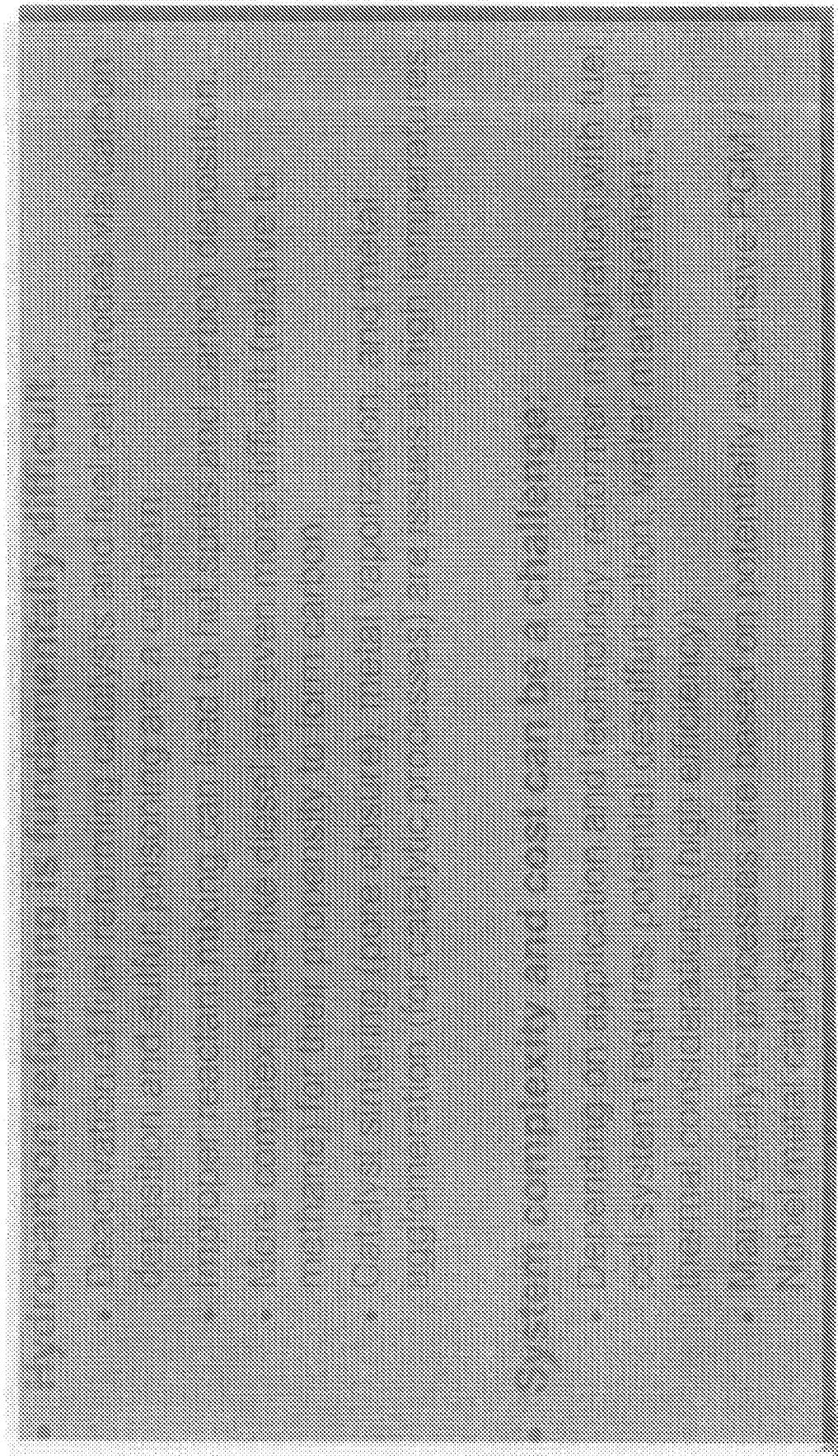
Fuel Processing Focus Area
Planning Assumptions – Core Program

Fuel Processing for SECA

General Approach for Sulfur Containing Fuels

S-Tolerant Reformer & FC Anode:

S-Fuel →

Oxidant →

Reformer (Partial Oxidation)

← Recycle

Fuel Cell Stack

Cathode

Anode
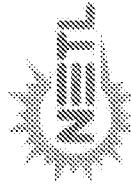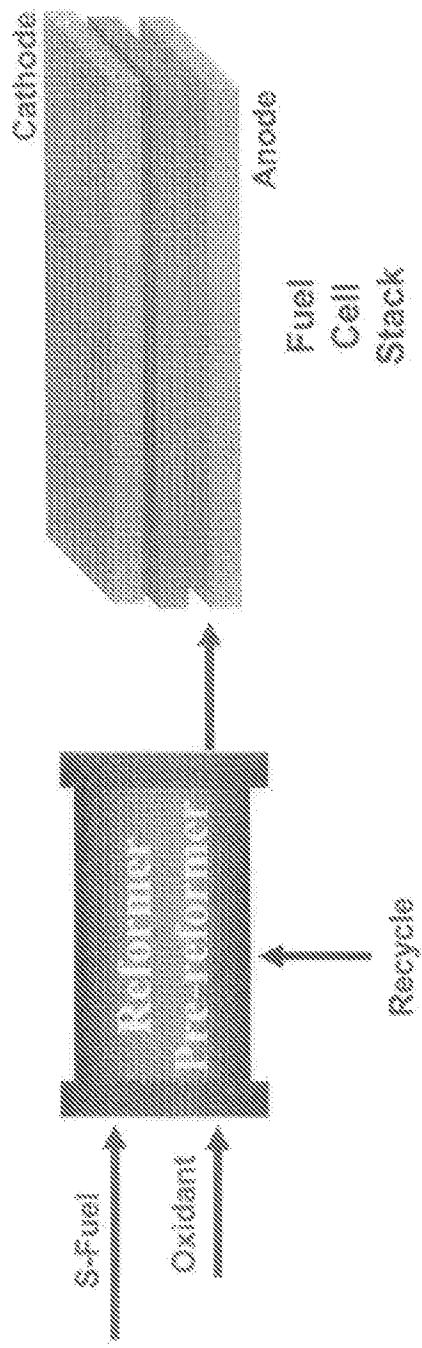
Fuel Processing for SECA

Reformer Nozzles – Reactant Mixing

Diesel

Air

Recyc. Exhaust

Reformate (H$_2$, CO, CH$_4$...)

Issues/Requirements:

- **Mixing Quality & Performance**
  - Requires intimate mixing to avoid unvented carbon / carbon precursor reactions or hot spots on reaction surface.
  - Turndown requirements may limit technology choices
  - Fraction distillation of multi-bp component fuels like diesel difficult (Need to avoid tar & carbon formation) Temperature control critical.

- **Recycle & Preheat**
  - Incorporation of high temperature anode recycle or preheated reactants non-trivial

NETL
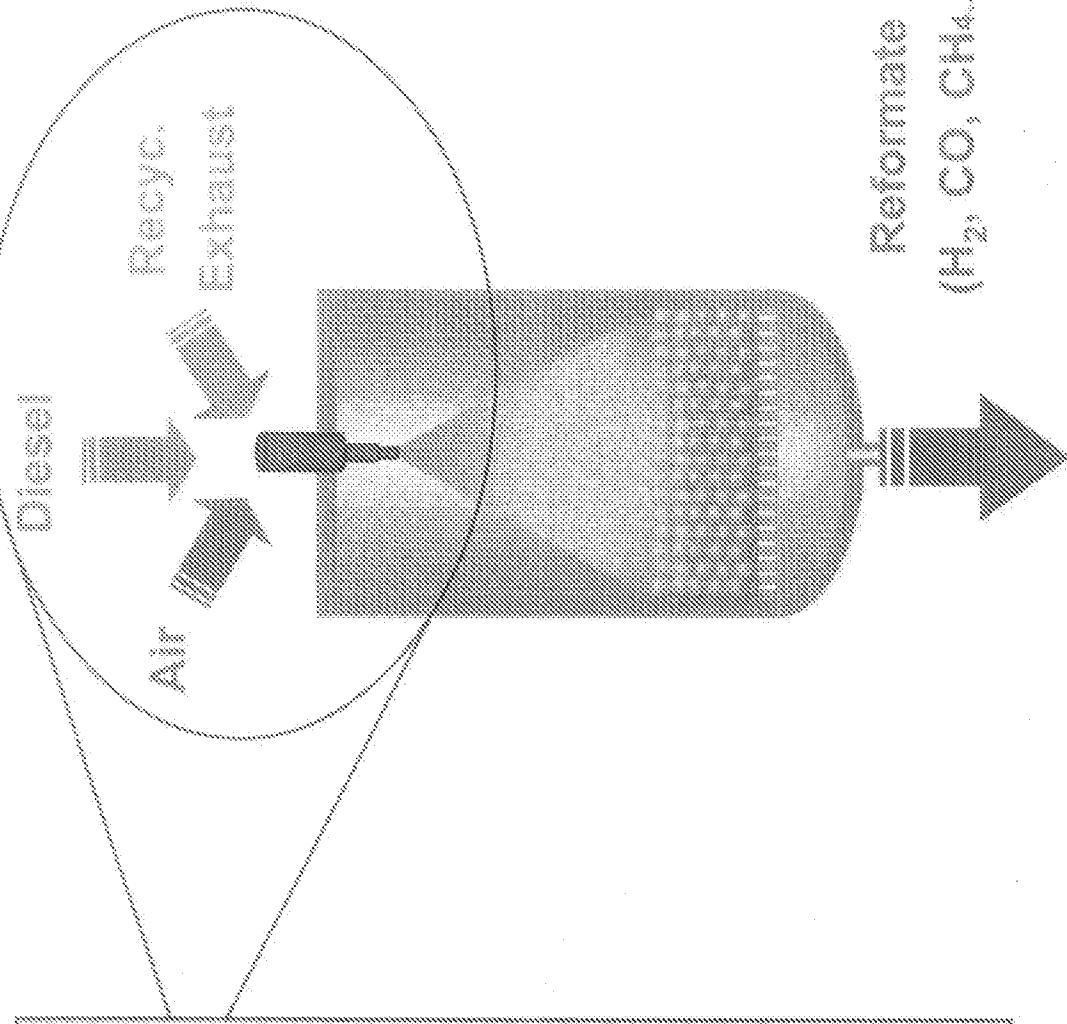
Fuel Processing for SECA
Reaction Media — Catalysts
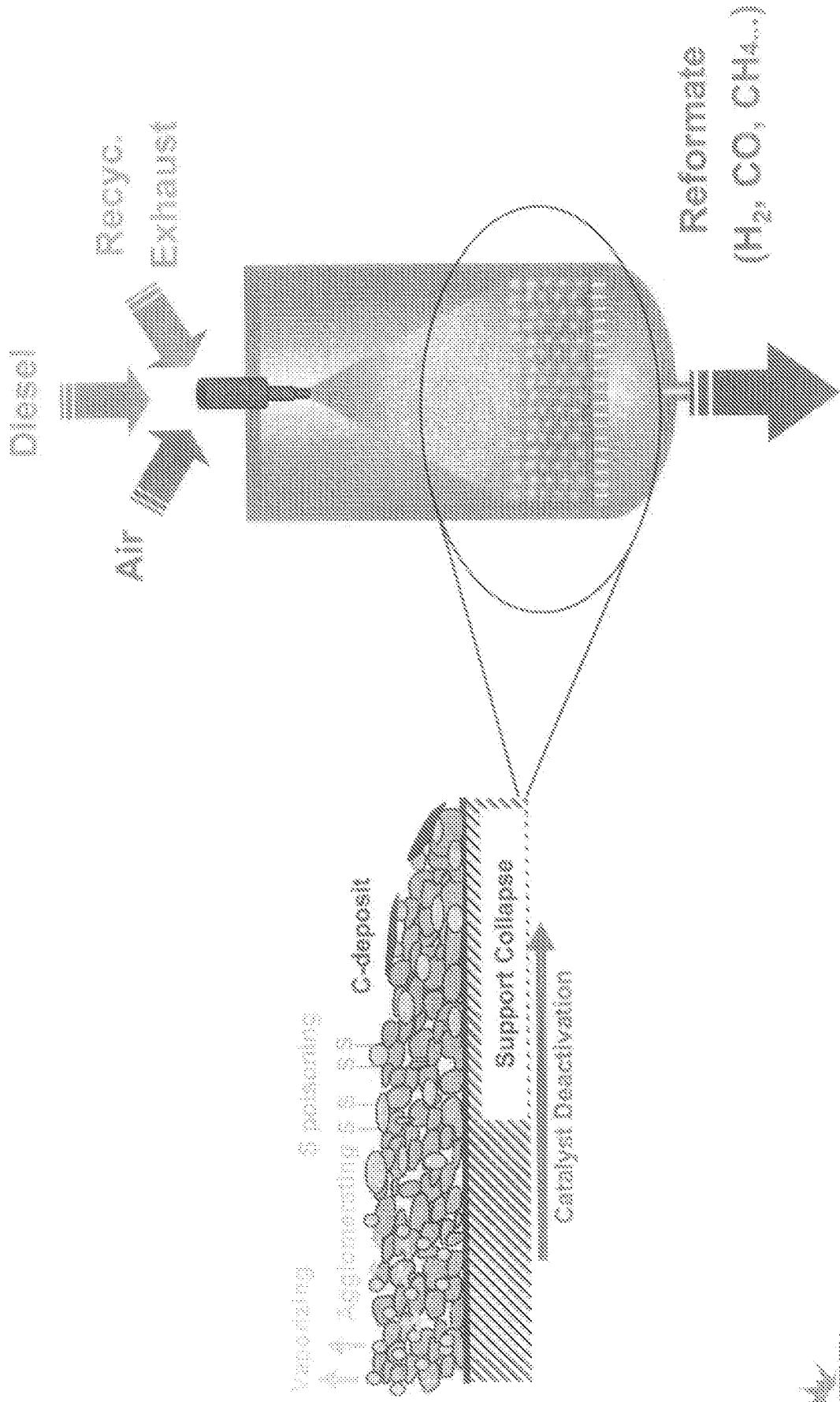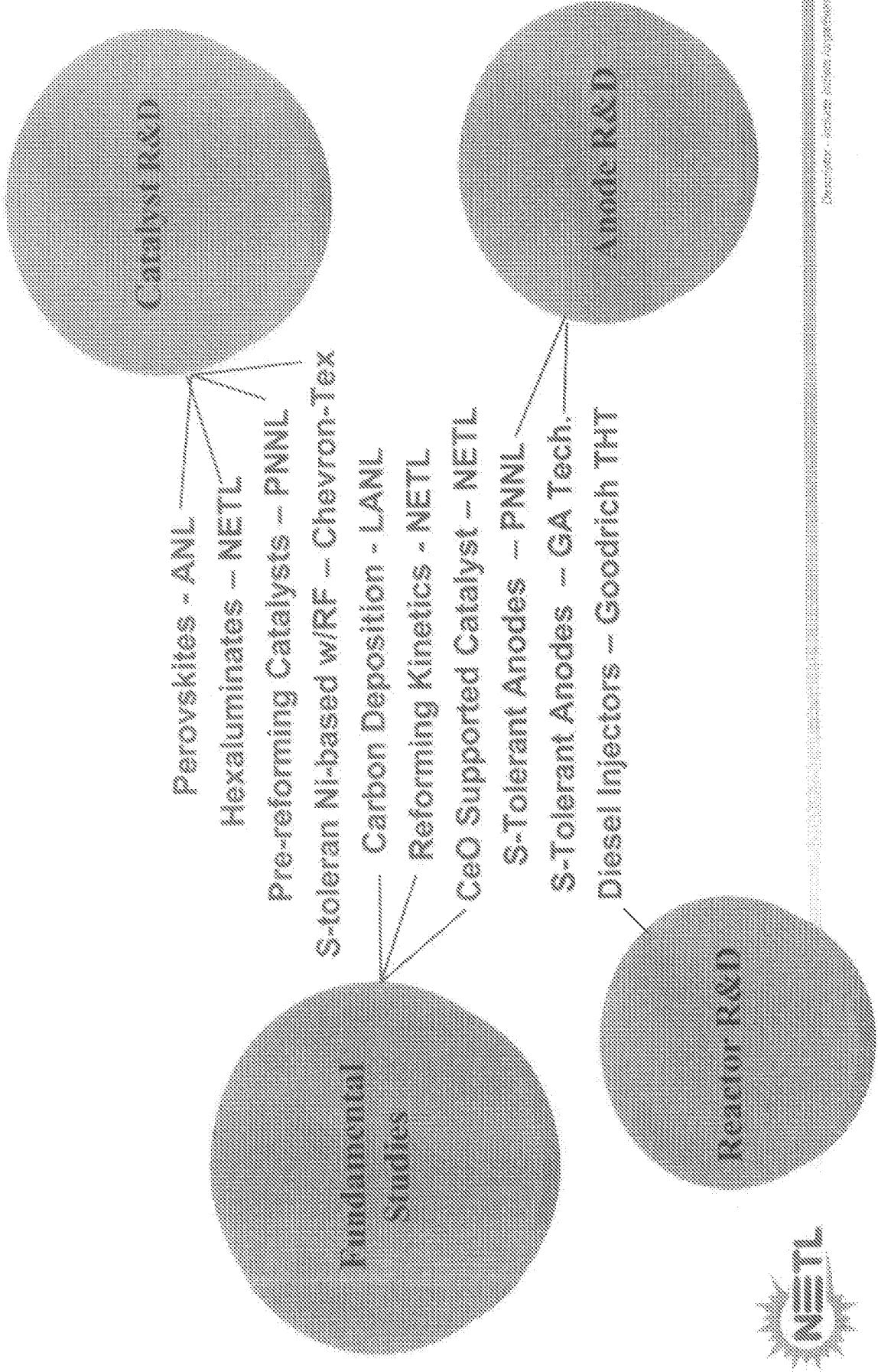
Diesel

Air

Recyc. Exhaust

Reformate
(H_2, CO, CH_4...)

Sintering

Agglomeration

S poisoning

C-deposit

Support Collapse

Catalyst Deactivation

Fuel Processing Focus Area
Current R&D Efforts in Core Program

Perovskites - ANL

Hexaluminates – NETL

Pre-reforming Catalysts – PNNL

S-toleran Ni-based w/RF – Chevron-Tex

Carbon Deposition - LANL

Reforming Kinetics - NETL

CeO Supported Catalyst – NETL

S-Tolerant Anodes – PNNL

S-Tolerant Anodes – GA Tech.

Diesel Injectors – Goodrich THT
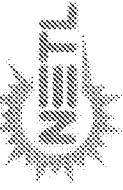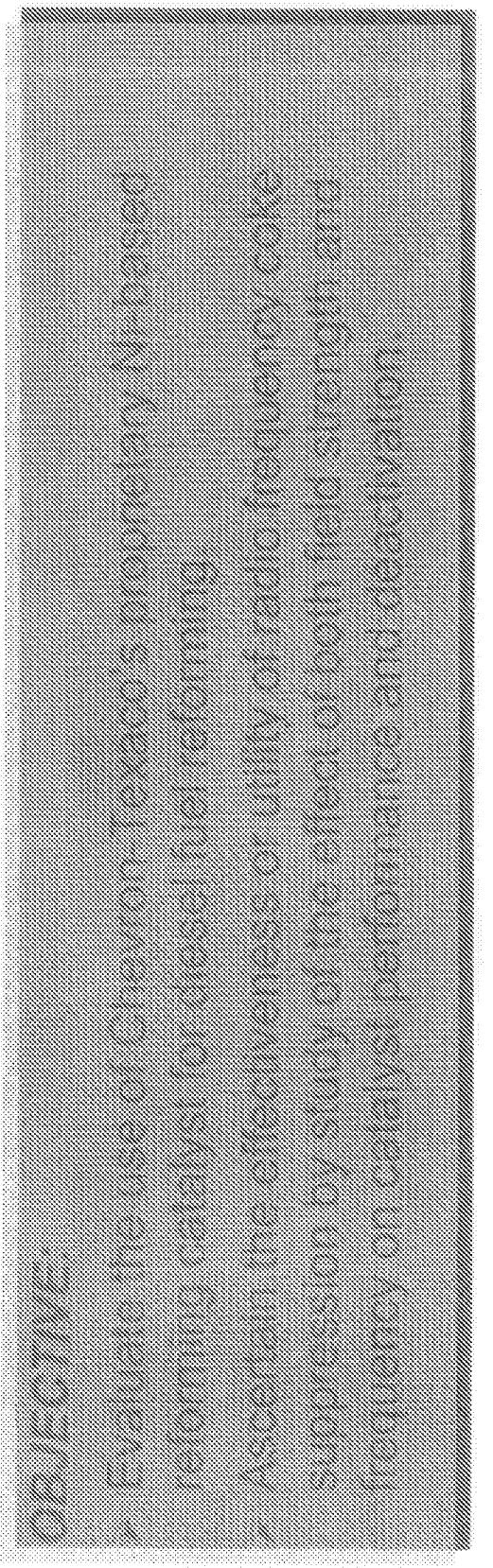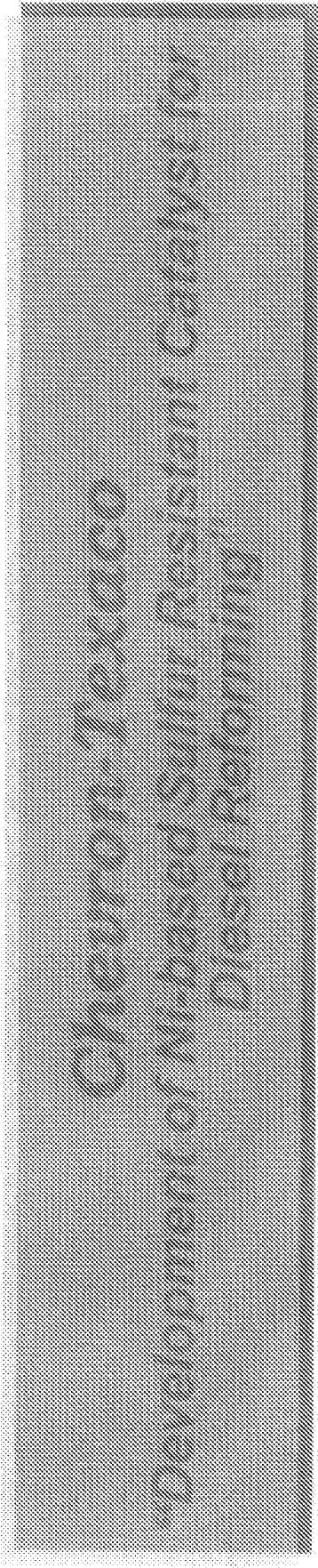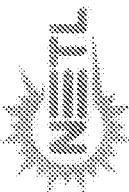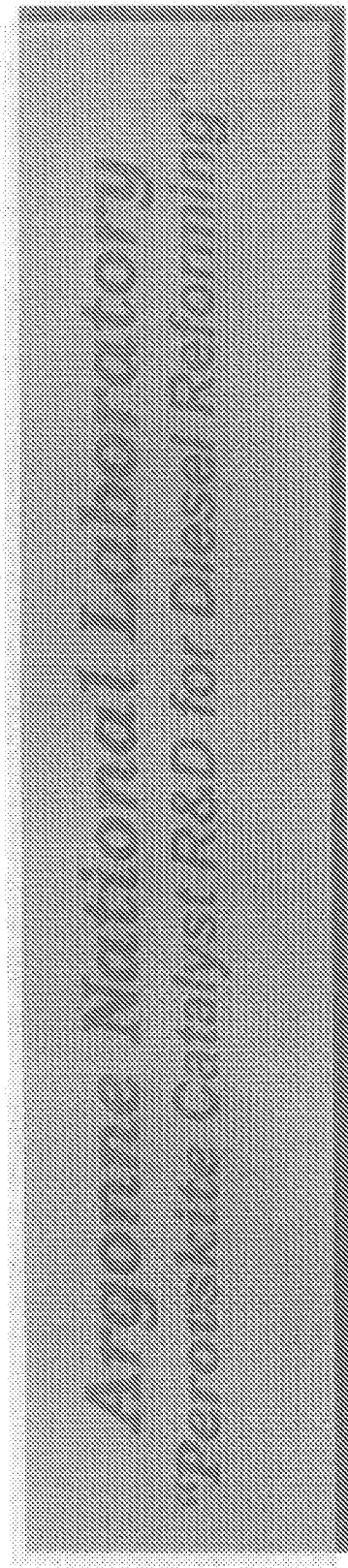
Current Active Projects
Fuel Processing – Diesel Reforming
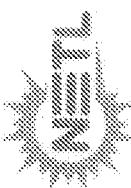
Current Active Projects
Fuel Processing — Diesel Reforming
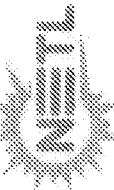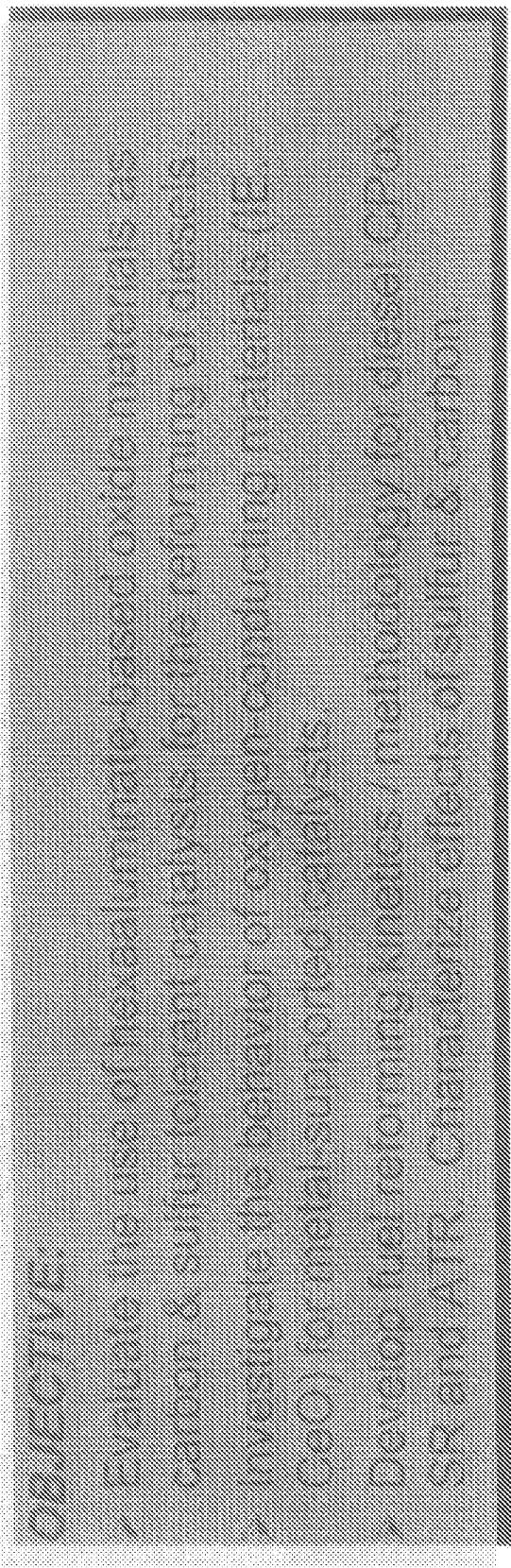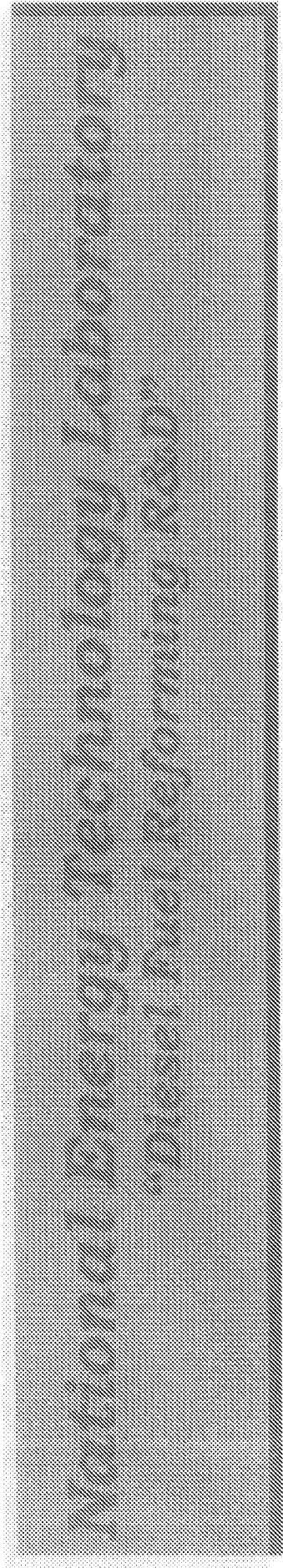
Current Active Projects
Fuel Processing — Diesel Reforming
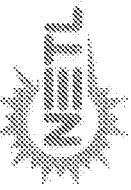
Current Active Projects
Fuel Processing — Diesel Reforming

Current Active Projects
Fuel Processing – Anodes

Current Active Projects
Fuel Processing — Reformer Injectors
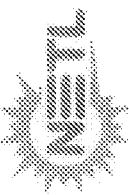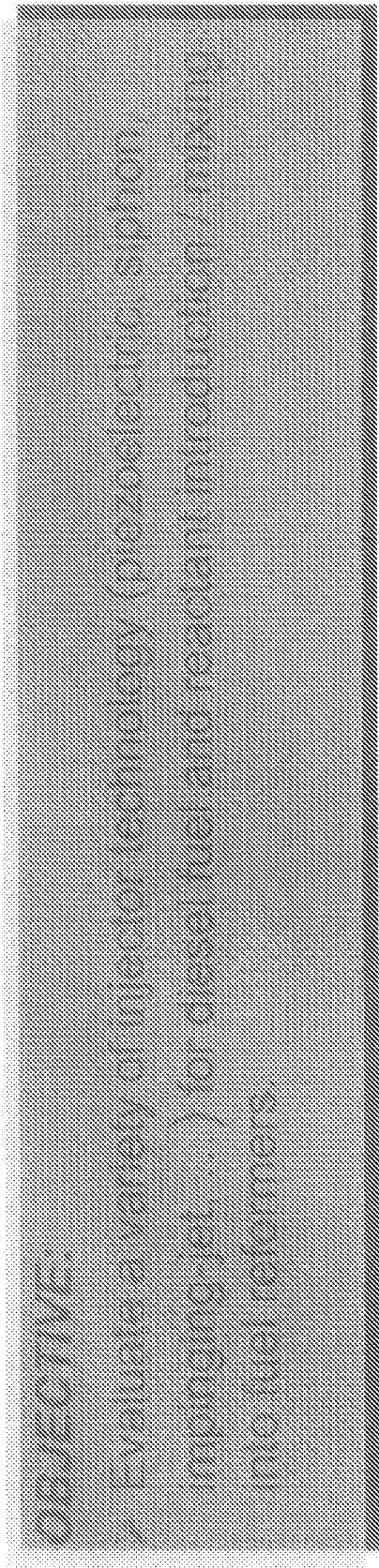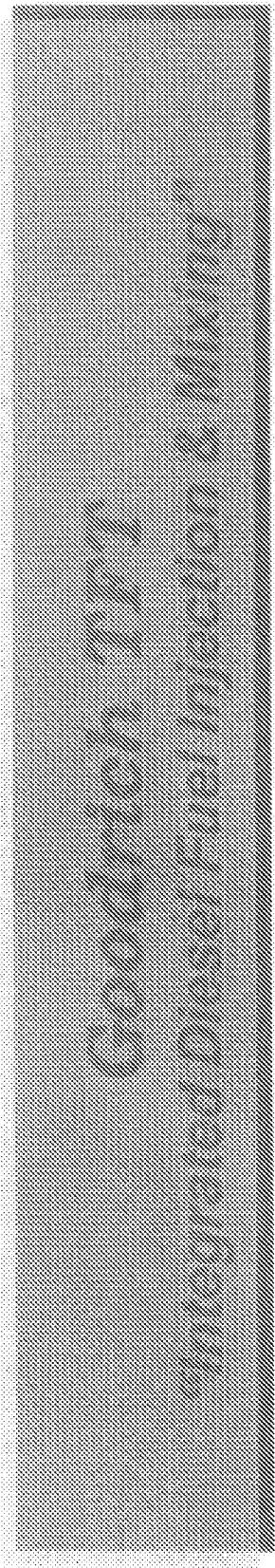
Current Active Projects
Fuel Processing – Anodes
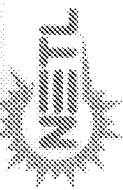
Current Active Projects
Fuel Processing — Desulfurization (SBIR)
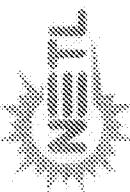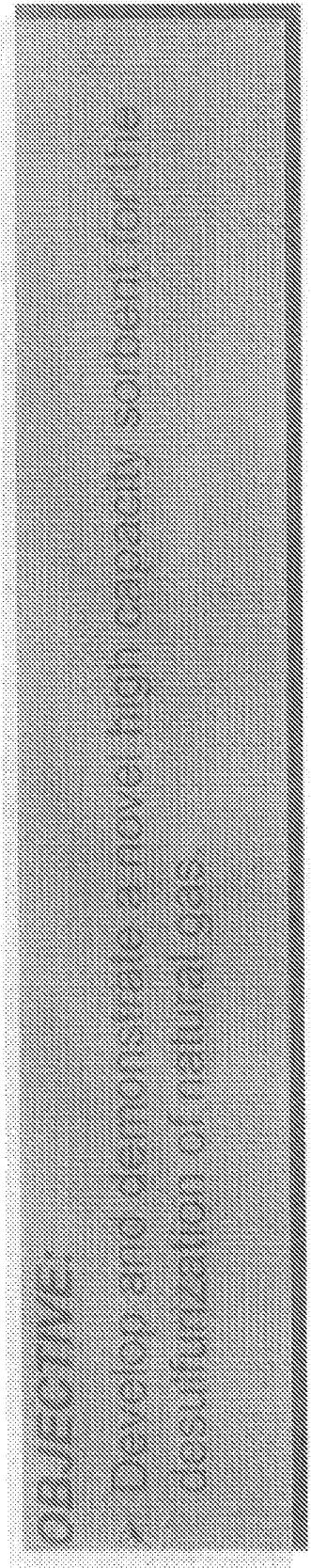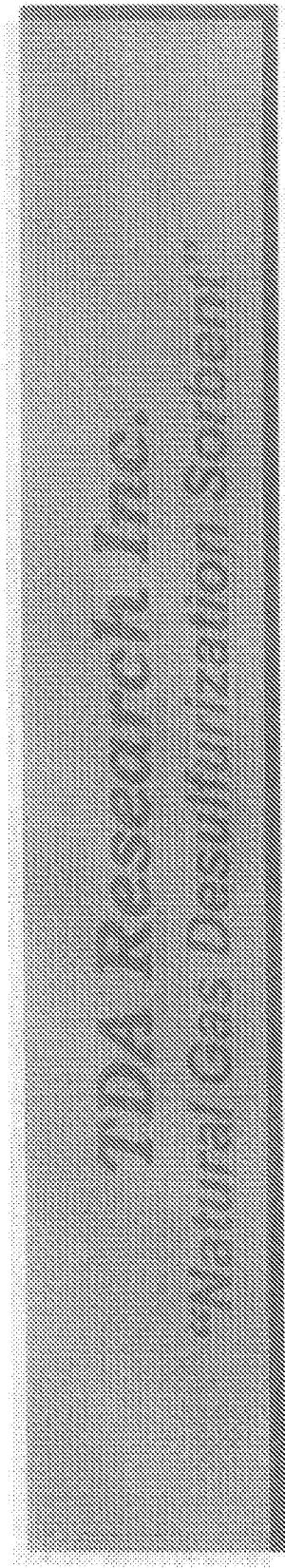
Fuel Processing Focus Area
Current R&D Efforts in Core Program
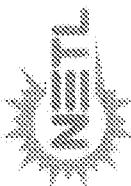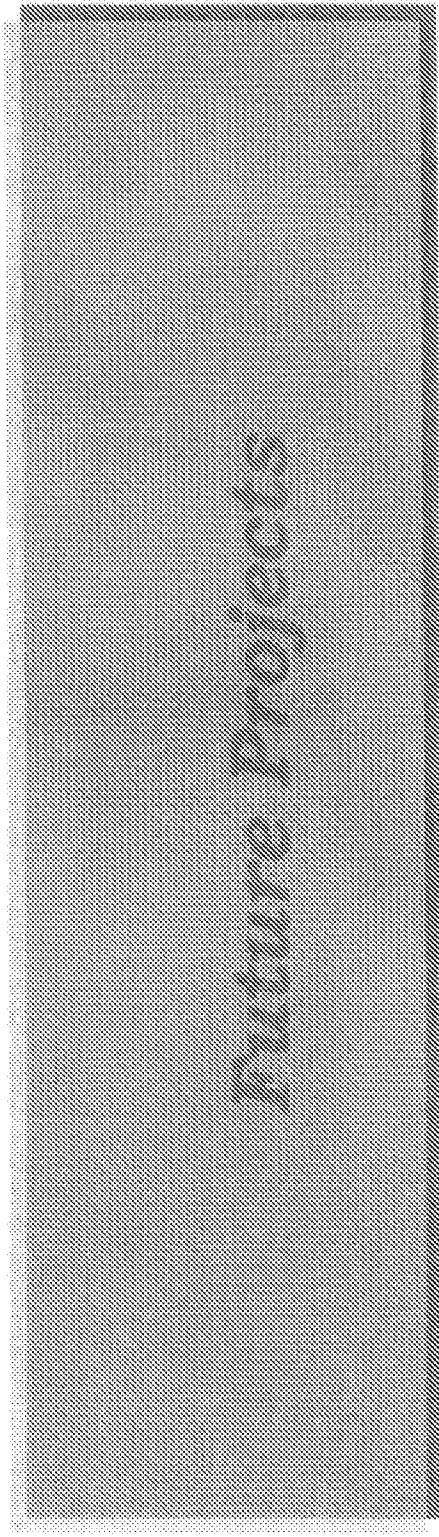
Fuel Processing Focus Area

Current R&D Efforts in Core Program

Focused on Materials & Fuel Processing:

- Seals
  - Rigid, High-Strength Sealing Concepts
  - Innovative Sealing Concepts

- Interconnect
  - Material for SOFC Cathode/Interconnect Interface
  - Identify/develop Interconnect Materials

- Electrodes
  - Infiltration of Active Elements into SOFC Electrode Structures
  - Quantification and Understanding of Cr Poisoning of Cathode Activity

- Fuel Processing
  - Sulfur and Carbon Tolerant Diesel Fuel Reformation Catalysts
  - Alternative Reforming Concepts
  - Technology for Logistic Fuel Applications

NETL

Fuel Processing Focus Area
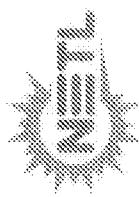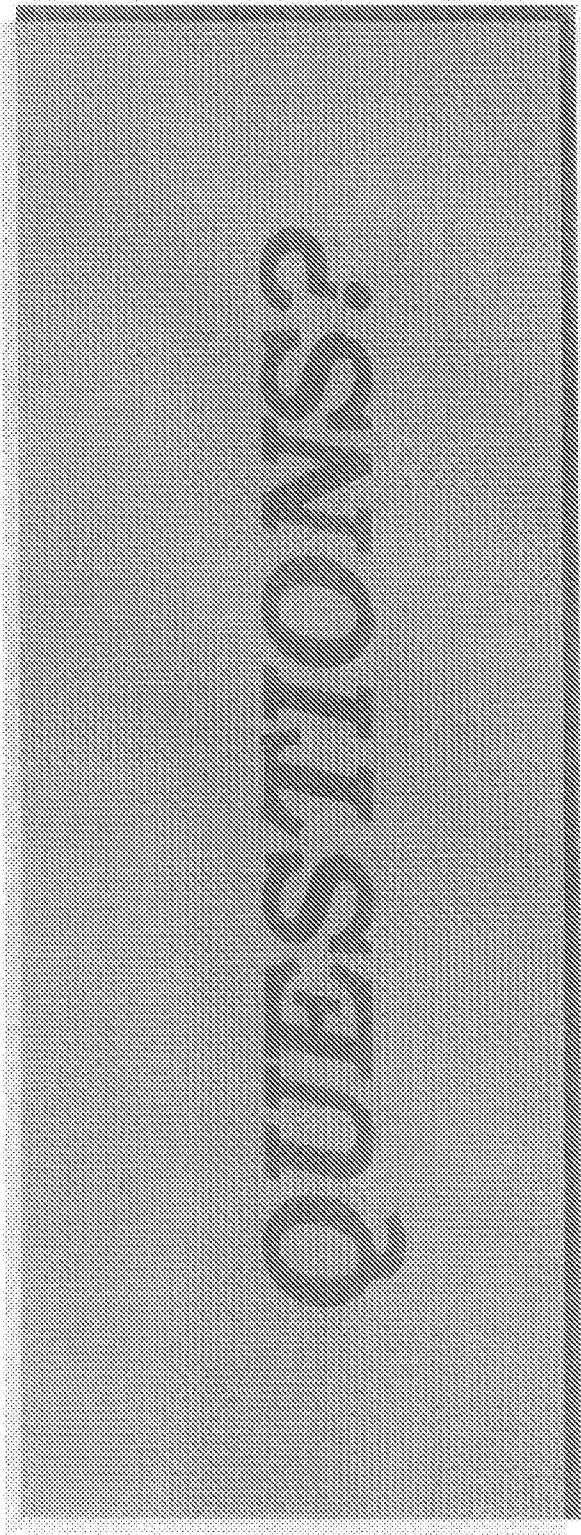
NETL On-site Fuel Cell Research